University of Wisconsin Milwaukee
UWM Digital Commons

Theses and Dissertations

December 2012

Copper Intercalation into Graphite

Kyle Kalbus
University of Wisconsin-Milwaukee

Follow this and additional works at: https://dc.uwm.edu/etd

 Part of the Materials Science and Engineering Commons

Recommended Citation
Kalbus, Kyle, "Copper Intercalation into Graphite" (2012). *Theses and Dissertations*. 34.
https://dc.uwm.edu/etd/34

This Thesis is brought to you for free and open access by UWM Digital Commons. It has been accepted for inclusion in Theses and Dissertations by an authorized administrator of UWM Digital Commons. For more information, please contact open-access@uwm.edu.

COPPER INTERCALATION INTO GRAPHITE

by

Kyle Kalbus

A Thesis Submitted in

Partial Fulfillment of the

Requirements for the Degree of

Master of Science

in Engineering

at

The University of Wisconsin-Milwaukee

December 2012

ABSTRACT
COPPER INTERCALATION INTO GRAPHITE

by

Kyle Kalbus

The University of Wisconsin-Milwaukee, 2012
Under the Supervision of Professor Benjamin Church

An electric brush is necessary for an electric motor to function. The purpose of this thesis is to propose a technique to improve electric brush properties in an effort to produce a more proficient electric motor by creating a new brush material with improved properties and performance. There are many applications for electric motors and each application would benefit from overall, increased proficiency. Understanding the role an electric brush plays within an electric motor is crucial to improving functionality. The proposed technique to create a novel graphite-copper material involves a two-step procedure that will intercalate $CuCl_2$ into the graphite structure, and then by chemical reduction, will reduce the $CuCl_2$ and result in the final products of copper and graphite. The proposed technique seeks to successfully increase the conductivity and wear properties of an electric brush by incorporating copper into graphite which will also enhance the properties of an electric motor. This thesis will detail the procedures of data collection and how to analyze results of the proposed technique. Expected results will also be discussed utilizing preliminary data collected utilizing XRD, SEM, TGA, and BET equipment. Finally, struggles and challenges of such a technique will also be discussed as well as plans for future work on the proposed technique.

© Copyright by Kyle Kalbus, 2012
All Rights Reserved

TABLE OF CONTENTS

LIST OF FIGURES

LIST OF TABLES

INTRODUCTION

This project incorporates improving the efficiency of an electric motor by changing its overall composition and look. Understanding how electric motors and brushes work are crucial towards the accomplishing the final goal of this project. An electric motor can be defined as a device which conducts current between stationary wires and moving parts, typically using a rotating shaft. Some common applications include alternators, electric motors, and electric generators. Brushes for electric motors usually contain Graphite or Carbon powder. Copper is used to improve the conductivity in applications that involve Direct Current (DC). An electric motor consists of these essential pieces: rotor, commutator, brushes, axle, field magnet, and a DC power supply. The image below shows a schematic of the various components found in an electric motor.

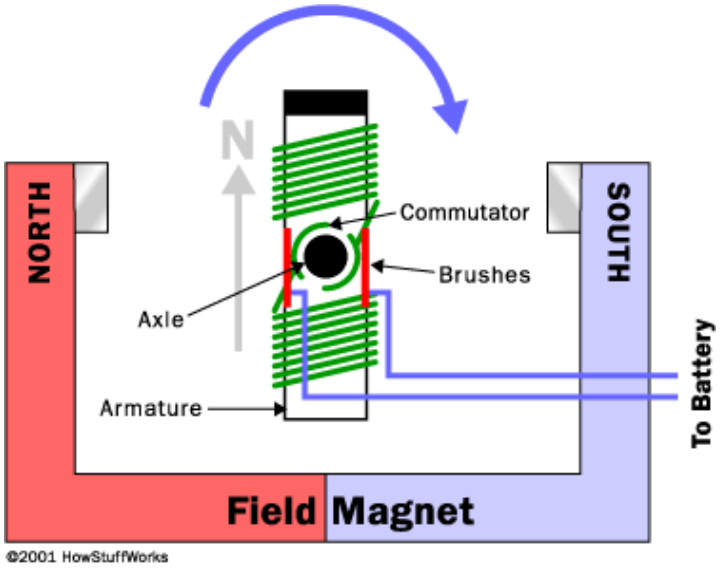

Figure 1: Schematic of an Electric Motor [1]

The magnetic field is created by the magnets at each end of the battery. The attractive and repelling forces from the magnets create a rotational motion that powers

the electromagnetic rotor. By fine-tuning and perfecting the cycle time of the electromagnet, it allows the motor to spin more freely. Individual components must also be explained. The armature is an electromagnet made by coiling a thin wire around two or more poles of a metal core and is attached to an axle along with the commutator. In the diagram below, it shows three different views of the armature.

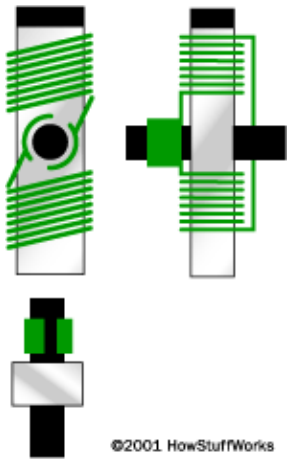

Figure 2: Three different views of an Armature. Left: front view, Right: side view, Bottom: end-on view. [1]

In the bottom image of the figure above, the armature part is not visible and this allows the focus to be on the pair of plates attached to the axle and these plates provide the connections for the coil of the electromagnet. The rotational motion of the electric motor is done by the commutator and brushes. The figure below shows how these components interact with one another.

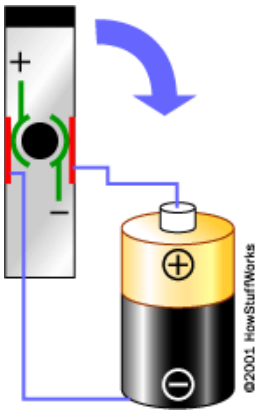

Figure 3: Shows how the Commutator and Brushes Interact with each other [1].

The commutator is attached to the axle of the electromagnet so they spin along with the magnet. The brushes, for this application are carbon, illustrated in red; remain in contact with the commutator. As current flows from the battery to the brushes, the charges between the poles change. When attractive charges begin to form between the battery and brushes, the electric field flips allowing electron transfer from the brushes back to the commutator.

As mentioned previously, electric motors use two electric brushes to transmit electric energy to the motor. The brushes are opposite in charge and complete an electrical circuit. The way they work is that the brush rubs on the commutator ring around the motor's armature. As seen in the figure below, this is what a typical carbon brush looks like.

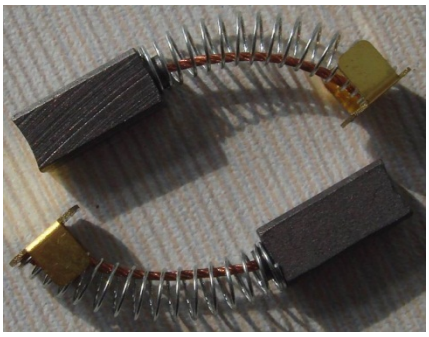

Figure 4: Carbon Brush for an Electric Motor [2].

As the image above shows, there are several different components involved in constructing a carbon brush. A copper wire is embedded within the carbon and the circular rotating piece of metal known as the commutator or slip rings are connected to the carbon. The copper wire brushes against the commutator rings and this allows a current to be conducted along the carbon brush.

The reason that carbon, more specifically graphite, is used is due to its properties of: low price, and conductivity. There is still enough resistance so that a gradual shift of current from the commutator can pass through each section. Brushes do have a tendency to wear out, but they are relatively inexpensive and simple to replace making it an attractive option for low end electric motor applications.

This project was initiated by Schunk Graphite Technology, LLC located in Menomonee Falls, Wisconsin. Schunk Graphite is one of the leading companies when it comes to carbon-based products in the world. This organization also manufactures more than carbon brushes. Other products include: bearings and seals, fuel cell plates, space technology equipment, along with several other very specialized applications [3].

The Research and Development Team at Schunk Graphite is looking for ways to improve the performance of the carbon brushes they produce. The question was posed: Does the type of graphite used in manufacturing carbon brushes have a significant impact on the performance of the component? Based on this question, the goal of this project was to determine if there was a way to improve the brush performance by creating a novel material of graphite with intercalated copper.

Barring that the answer to be yes, the purpose of this project became to improve the conductivity and wear properties of electric brushes. For carbon brushes, copper is

commonly used to improve the conductivity. Graphite, which is how carbon is naturally found, has a hexagonal structure. The idea is to get copper atoms into the carbon structure and form an intercalated material with copper located between the layers of carbon. This intercalated material is not commercially produced and has not been attempted for applications that requires a high conductivity and wear resistance.

The stages of Graphite Intercalation Compounds are labeled as Stage 1, Stage 2, etc. and it is used to identify the layers of graphite between a layer of intercalate. Properties such as composition, temperature of formation, molar ratios, and particle size are all unique in this regard with respect to each other [4-7]. For copper intercalation, the number of graphite layers sandwiched by layers of $CuCl_2$ determines the stage of the intercalation. The figure below depicts what the different intercalation stages would look like. As shown in Figure 5, the A, B and C layers are the different graphite layers.

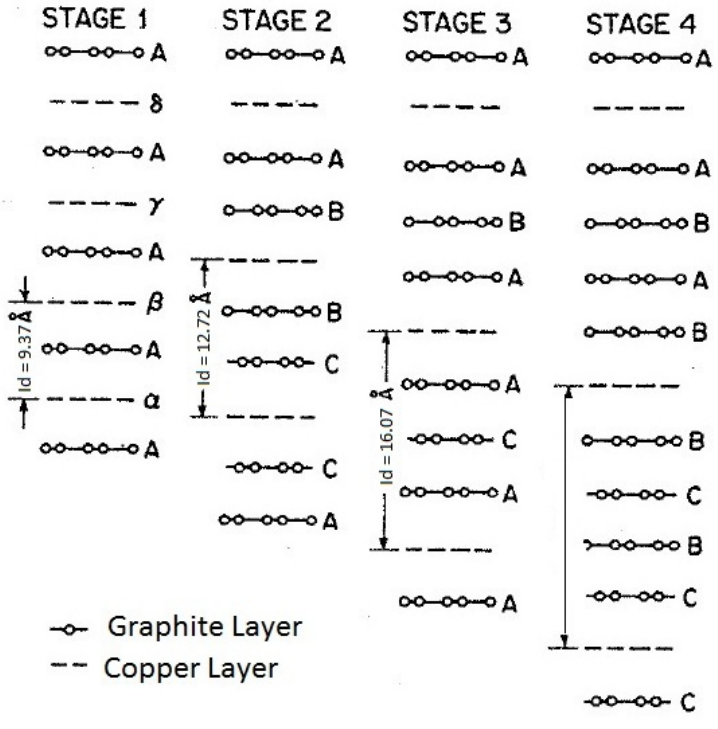

Figure 5: Example of Different Staging Levels of Intercalation [4]

The layers labeled α, β, γ, and δ characters represent the intercalation layers, which is copper in the figure above. For Stage 1 intercalation, the figure above shows that there is one layer of graphite between the copper layers, or alternating layers of copper and graphite [4]. Looking along the side of the figure, there is an I_d given, which is known as the intercalation distance. The intercalation distance is the distance between two copper layers in the graphite structure. For Stage 1, Stage 2, and Stage 3, the intercalation distances (I_d) are 9.37Å, 12.72Å, and 16.07Å [5, 6].

In was discovered by Inagaki and Ohira that the optimal formation of Copper intercalation is at 450^{o}C for three days [8] and is considered the standard practice as the initial step to get Copper intercalated into the graphite structure. The result of this process is a Stage 1 Graphite Intercalated Compound with intercalation of $CuCl_2$. The ratio of graphite to anhydrous $CuCl_2$ mixed together is done in a 1:1 molar ratio. After mixing the graphite and $CuCl_2$ and taking it out of the furnace, the resulting material is washed in diluted HCl solution and then with H_2O to remove the excess $CuCl_2$ and then the powder is dried in a vacuum oven at 60^{o}C.

Below are some prior results from a group that took a different approach in eliminating the chlorine atoms from the structure. Ammonia, distilled H_2O, ethylenediamine, KB_4, ethanol, distilled H_2O (again), and finally HCl acidified $FeCl_3$ solution was used to remove the loose Copper species.

Taking a look at the planar view below, one can see what a Stage 1 Copper GIC structure looks like [4]. There is alternating layers of Graphite, which is hexagonal in shape and the CuCl2 intercalated layer, is represented by the circles.

The table below shows the results of all stages of Copper intercalated graphite

using the molten salt method [5, 7]. The formation temperature increases as the stage increases, especially for stage 3 formation. The chemical composition changes significantly as well. Stage 1 produces the highest amount of copper within the structure, but also has the highest standard deviation [7]. Stage 2 and Stage 3 have a lower amount of copper within the structure as would be expected, since it forms less frequently among the graphite planes. The sizes of the copper particles are relatively constant throughout the different stages. Stage 1 particles had an average size of 22.5nm, whereas Stage 2 and Stage 3 particles were almost identical in size being 28.3nm and 28.5nm [7]. The higher amount of variation in Stage 1 compared to Stage 2 and especially Stage 3 shows the heterogeneous nature of the structure. Stage 1 has the highest standard deviation and the size of the copper molecules vary significantly. Stage 2 is a lot more consistent and homogenous than Stage 1 looking at the results, but it is not quite as homogeneous as Stage 3 results show [7].

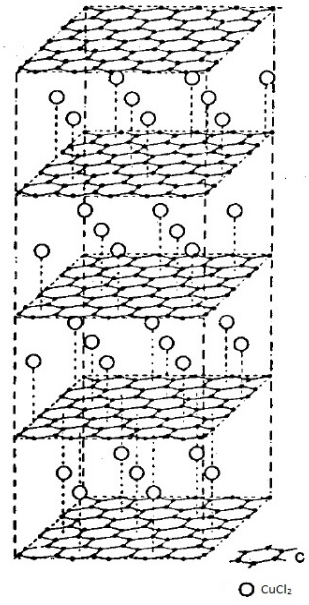

Figure 6: Planar view of Stage 1 Copper GIC. [4]

Sample No.	Precursor	Chemical composition[a]					Size of copper (nm)		
		Element	C	Cu	Cl	K	Min.	Max.	Average
1	Stage 1 GIC Formed at 300 °C	Content (wt %)	68.71	18.85	4.30	8.13	7.2	51.8	22.5
		SD[b]	7.29	1.83	2.15	1.82			
2	Stage 2 GIC Formed at 320 °C	Content (wt %)	72.02	12.87	4.43	10.68	15.8	58.3	28.3
		SD	1.37	1.05	0.26	0.66			
3	Stage 3 GIC Formed at 450 °C	Content (wt %)	72.80	11.39	4.17	11.64	18.9	37.9	28.5
		SD	1.75	0.49	0.25	1.23			

[a] The product compositions were characterized using EDX; the concentration of boron in the samples was only a trance amount and was omitted here. [b] SD: standard deviation.

Table 1: Intercalation Results from a Recent Paper to Show the Relationship between Stage and Composition [7]

METHOD

This project hopes to accomplish two steps. The first step is to get the copper atoms in the carbon structure and by mixing anhydrous copper (II) chloride with natural graphite in molar ratios of: 1:1, 3:1, and 6:1 that are in powder form [5]. These powders are then placed into a glass ampoule, where the air will be removed from and vacuum sealed because anhydrous copper chloride reacts strongly to air adsorbing moisture from the atmosphere, lowering the reactivity of the copper chloride and restricting the amount of material that can intercalate into the carbon layers.

After the powdered mixture is sealed in an ampoule, it is time to heat the ampoule in a tube furnace at 480^{o}C for three days [5, 8]. After the ampoule has been removed and the material within it has been recovered, the recovered material will be cleaned. This is done by washing the solute in diluted hydrochloric acid and water to remove the remaining copper chloride. The resulting material is then dried in a vacuum oven at 60^{o}C for at least 12 hours to remove any moisture that remains from the washing process.

The resulting material left is the graphite that has the copper intercalated in it. Even with the washing, there are still excess chlorine atoms within the structure. To reduce this excess, the powder can be loaded into a watch glass and processed with 4% Hydrogen in Argon (4% H_2/Ar). This is done within a tube furnace at 300^{o}C for an hour. This process will be optimized using TGA to study the weight change kinetics applied to the tube furnace.

There are several primary methods that can be used to determine the effectiveness of this process by collecting data after each step. Thermogravimetric Analysis (TGA) will be used to determine the mass change. X-Ray Diffraction (XRD) will be used to

determine the secondary components in each graphite sample and to measure the relative amount of intercalation that took place. Brunauer-Emmett-Teller (BET) Surface Area Analysis will be used to analyze the changes in surface area and porosity of the graphite and the graphite intercalated compound (GIC). Finally, the Scanning Electron Microscope (SEM) will be used to closely examine the microstructure of the graphite samples and the GIC compound along with Energy Dispersive X-Ray Spectroscopy (EDX or EDS) that will determine impurities present.

RESULTS

Thermogravimetric Analysis (TGA) measures the amount and rate of change of mass within a carefully controlled temperature and atmosphere. This is used to determine the composition and to predict the thermal stability resulting from changes due to decomposition, oxidation, or dehydration [9]. The goal of TGA in this project is to use this method to determine the amount of copper intercalated within the graphite structure. In order to show the amount of copper intercalation, the curves of the raw graphite will be compared to and the intercalated material following each step of the process to see the presence of copper.

The simplest and most effective way to accomplish this is by coming up with a heating program that burns off all the graphite powder. In Nitrogen gas, the boiling point was initially thought to be between 700-800^{o}C. The program that was initially done was to ramp the temperature up 20^{o}C/min up to 1200^{o}C and hold that temperature for ten minutes to ensure that all the powder evaporated entirely. The ramp rate had to be reduced to 15^{o}C/min to ensure that all the graphite evaporated before the end of the TGA run.

Below is a figure of the TGA results for the pure graphite samples. The table shows the important data that can be obtained by running a TGA sample. The onset temperature is the point at which significant mass change occurs. The derivative onset temperature is slightly different than the regular onset temperature because the measurement is taken from the derivative curve of the TGA result. The mass change is the difference in mass percent from start to finish, and represents the percentage of mass that was lost during the TGA sample run [10].

Type	Onset Temp(^{0}C)	Derivative Onset Temp.(^{0}C)	Mass Change
F11	698.2	703.5	96.98
F99.5	698.7	710.8	98.29
Micrograph 99835	744.3	731.4	96.59
Timcal KS75	770.8	796.0	97.57
Timcal M150-97	790.5	760.2	96.76
Timcal T44	765.5	744.1	98.93

Table 2: TGA Results for the Raw Graphite Samples

The F11 and F99.5 both have very similar temperatures and mass changes. The Timcal materials have a similar grouping as well with the onset temperatures being very close to each other. The relative mass change for all these are relatively close to each other. One of the bigger sources of error is mass size. Basically, the bigger the sample size, the lower the percentage of material gets burned off. The reason is that the mass loss ends shortly before the maximum temperature is reached, so there may be some additional burning if we let this continue.

Below are the two of the most different TGA curves that came out through the characterization process. Figure 1 is displaying the F11 TGA curve. The vertical axis is %TG and on the right side is the scale for the derivative curve for the TG. The onset temperature where the material starts to burn off is approximately 700C with a mass change of 97%.

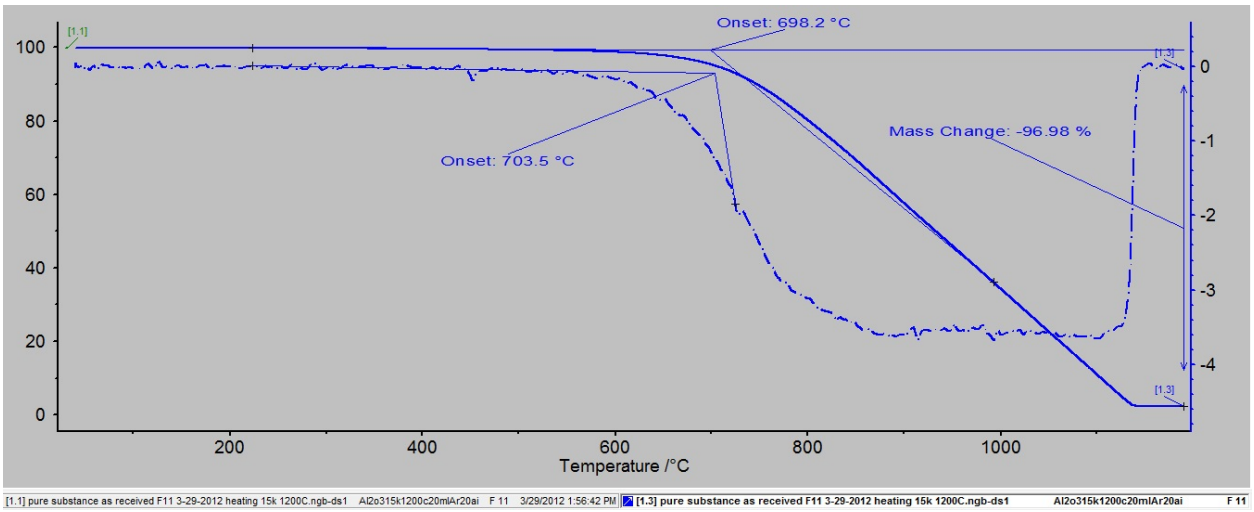

Figure 7: TGA Results from F11 raw material

Compare the sample of F11 to that of Figure 2 below which is the Timcal T44. The onset temperature takes place at approximately 750C and has a mass change of almost 99%. The evaporation rate of the T44 is quite a bit greater than the F11 and takes place during a smaller temperature window.

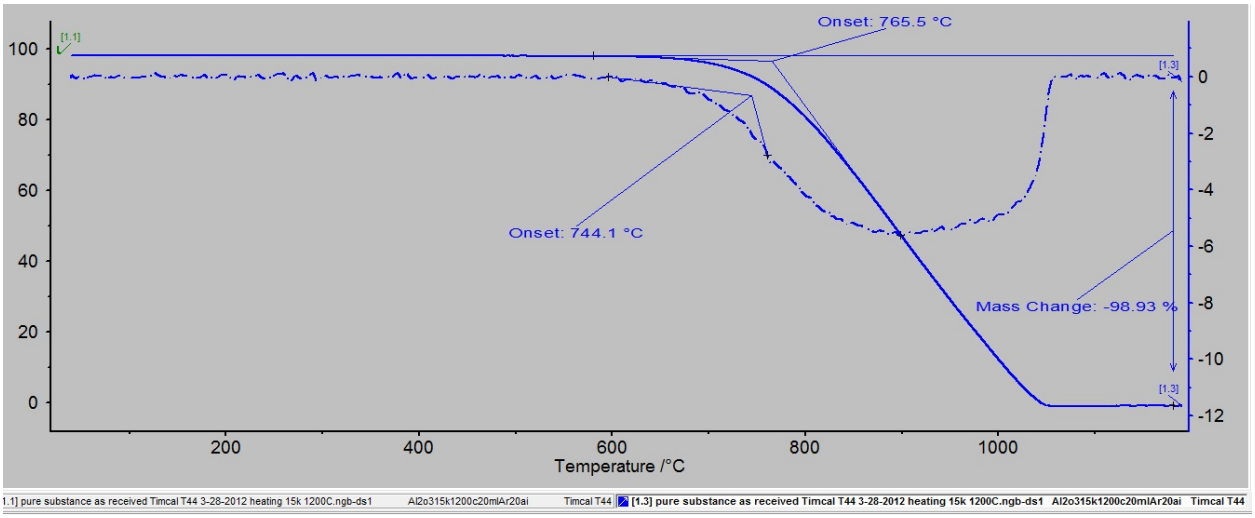

Figure 8: TGA Results from Timcal T44 Raw Materials

It looks like the Timcal T44 starts to burn off 50C higher than the F11 and finished evaporating at 1050C whereas the F11 continued the process until about 1100C. This is likely related to the Carbon purity of the two raw materials. The percent carbon of

the F11 is 97.90% whereas the content in the Timcal T44 is somewhere in the lower 99% range. This would explain why the onset begins sooner in the F11 and lasts to later temperatures than the T44 due to the impurities.

X-Ray Diffraction (XRD) is a way to determine the phase identification of a crystalline material and can provide information on unit cell dimensions. The analyzed material is typically found in a powder form and the average bulk composition can be determined [11]. X-Rays are reflected off of the sample from different atomic layers from various angles and the peaks with respect intensity and angle of two-theta can be used to determine the crystal structure, lattice parameters, and the relative composition of an unknown material. The graphite powder analyzed during this project had different levels of purity, ranging from 95-99% depending on the sample. When natural graphite is being pulled from the earth, there is a material called fly ash that comes out with it and is a combination of several different ash byproduct materials such as SiO_2 and Na_2O. The best way to describe an ash is any oxide naturally found in the earth.

For this project, the goal was to use XRD to determine the approximate amount of intercalation that occurred. The graphite powders were run with a general scan of two-theta from five to 70 degrees continuously at a rate of 1.25 degrees per minute. This was done to get a general outlook of the spectra that resulted, and to determine if any of the ash content was detectable using XRD. There were some troubles getting a run to complete since the counts on the intensity maxed out, which made the rest of the run irrelevant. To fix that, the two-theta angle of 25.5 to 27 degrees was skipped due to the incredibly high peak from the graphite making the secondary peaks very small in size. This helped to reveal the secondary peaks from the XRD test, and the current was

amplified to help magnify the peaks. Below are the XRD patterns stacked on top of each other, and this was done to identify the differences between and identify what was the cause of them.

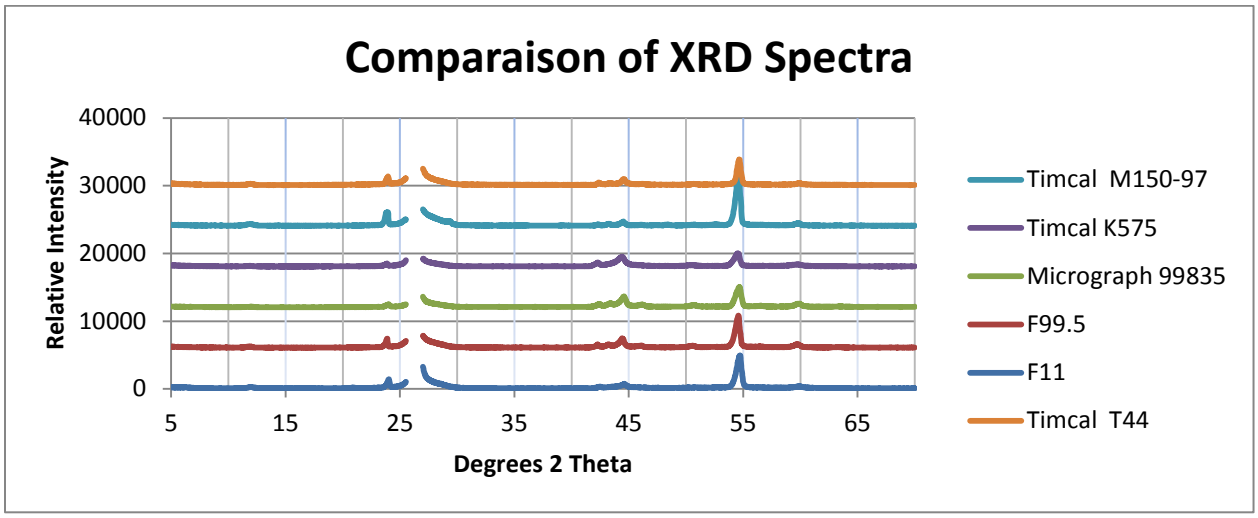

Figure 9: XRD Patterns of Raw Graphite Samples

The results from the XRD data show several spots that are worth inspecting. The peaks at the two-theta angles of 24, 42, 44, and 55 are the areas of interest since they vary by the material. After the peaks were identified, the XRD PDF cards compared the peaks to each other. The difficulty during this step is that the relative intensities are all based in relation to the strongest peak, which was skipped over to reveal the secondary peaks. So considering that detail, the two-theta angles where the peaks occur have an elevated emphasis for analysis over intensity. Below is an example of a graphite XRD pattern result superimposed on a PDF card for graphite. There were approximately 12 different PDF card results for graphite, so the best overall result was used to match up with the pattern.

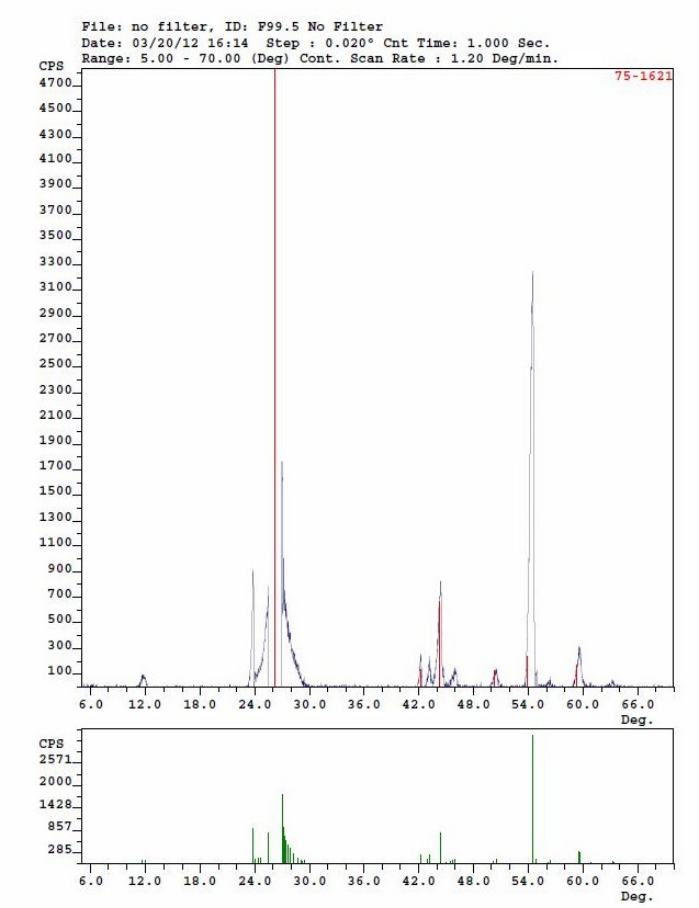

Figure 10: XRD Pattern with PDF Card 75-1621 [12] super-imposed on F99.5 graphite result.

As the figure above shows, the angles of the diffraction pattern match up very well. The intensities were quite accurate as well. The only peak that stands out is the one at about 55^{o} two-theta, and the fact that the biggest peak was skipped over to analyze the secondary peaks could have created this accentuated peak. The next step was to see if the major kinds of ash such as SiO_2 or Na_2O can be identified in the XRD pattern. After some analyzing and searching peaks, none of the types of ash or any other impurities could be found using this technique.

Results from the Brunauer-Emmett-Teller (BET) Surface Area Analysis are shown in Table 1. BET measures the specific surface area of a material by using physical adsorption of gas molecules on a solid surface [13]. The pore volume and diameter were

calculated using the Barrett-Joyner-Halenda (BJH) Adsorption. The BJH method, proposed in 1951, was designed for relatively wide-pore adsorbents with a wide pore size distribution. It turns out that it can be applied to nearly all types of porous materials. The model is based on the assumption that pores have a cylindrical shape and that pore radius is equal to the sum of the Kelvin radius and the thickness of the film adsorbed on the pore wall [14].

The results show that all the graphite samples are very porous. In the table below, the results show that the Specific Surface Area (SSA) is between 0.93 and 7.83 m^2/g which is a large area for one gram of material. The pore volume determines the amount of porosity per gram of material. The pore diameter is a measurement of the average pore diameter. The pore results are slightly narrowed by restricting the size of the pores between 17 Å and 3000 Å for the diameter.

	Specific Surface Area (SSA)	**Pore Volume**	**Pore Diameter**
Sample	**(m^2/g)**	**(cm^3/g)**	**(Å)**
F99.5	4.21	0.0133	118.6
Timcal KS75	4.96	0.0160	129.5
F11	7.83	0.0173	143.7
Micrograph 99835	2.88	0.00443	168.2
Timcal T44	4.04	0.0172	237.7
Timcal M150-97	0.93	0.00253	494.1

Table 3: BET Results for Raw Materials

Below are figures showing the isothermal plots of the F-11 and F-99.5 isothermal plots. There are two curves, adsorption and desorption that show the relationship between

the relative pressure and the quantity adsorbed. This relationship shows the amount of porosity of the different types of graphite.

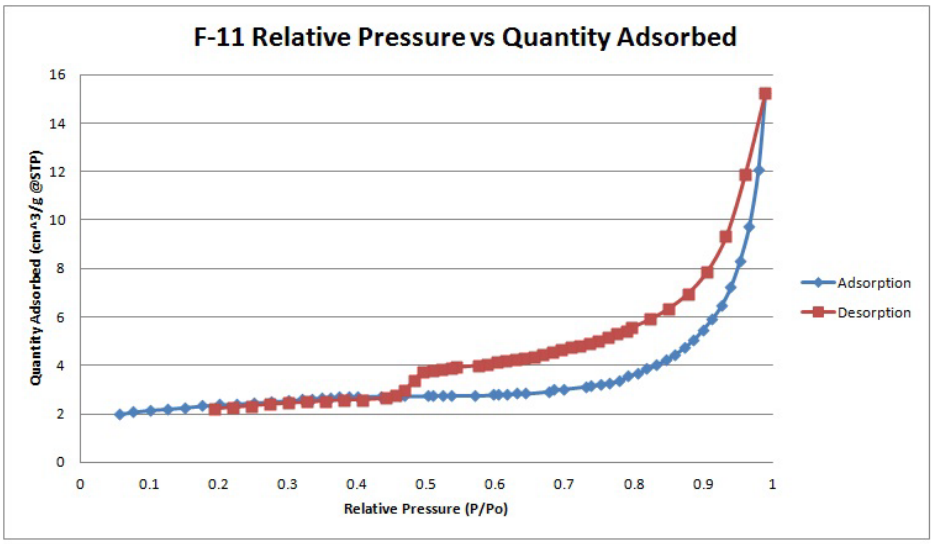

Figure 11: Isothermal Curves for Adsorption and Desorption of F-11

The results from the F-11 curves show some difference between the adsorption and desorption isotherms. The result that followed was expected since the surface area, pore size, and pore diameter are bigger than the other raw materials that are being compared.

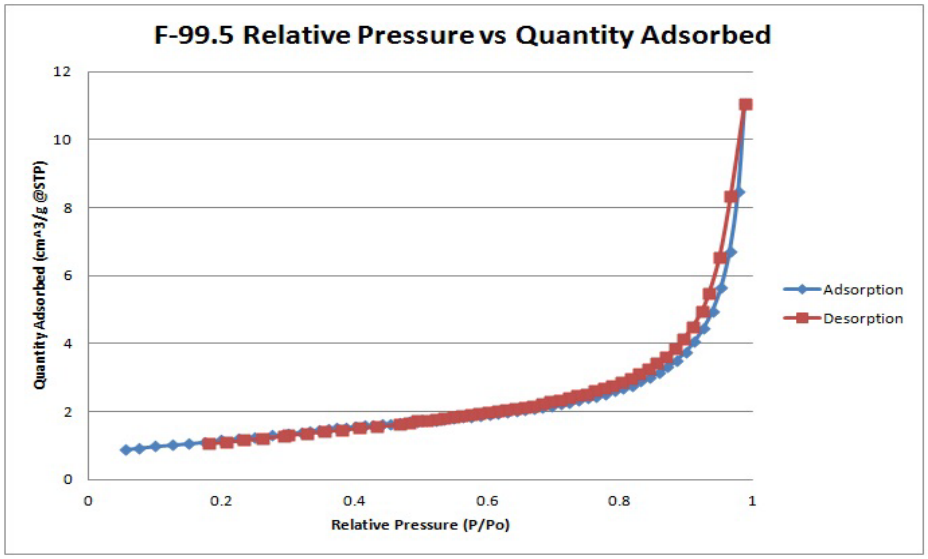

Figure 12: Isothermal Curves for Adsorption and Desorption of F-99.5

The results in Figure 12 the F-99.5 show the adsorption and desorption curves almost on top of each other which indicates minimal porosity within the graphite. The F-99.5 results from the table above shows that the powder has a lower surface area, pore size, and pore diameter, which would lead to closer adsorption and desorption curves. The higher surface area and pore size would probably make gas-phase transport and reaction easier. So this initial result indicates that the F11 should be a better starting material than the F-99.5. All the other graphite raw materials, not pictured, follow this shape. Overall, the higher surface area and pore size causes a higher amount of adsorption for the F-11 compared to the F-99.5 as well as a greater discrepancy between the relative adsorption and desorption curves between these two samples.

A scanning electron microscope (SEM) creates an image by scanning the surface of the sample with high energy electrons. The interactions that take place between electrons from the electron microscope and the sample reveal information about the sample including external morphology (texture), chemical composition, crystalline structure, and orientation of the sample being analyzed. Pictures were taken of each sample at various magnifications and at two different operating distances to better understand and to visualize the structure.

Low magnification gives insight of what the surface layers of the material look like and higher magnifications can be used to investigate how layers stack on top of each other and are orientated with respect to each other. The graphite samples were looked at two different operating distances as well. The closer working distance shows depth of field and can be used for Energy Dispersive X-Ray Spectroscopy (EDX or EDS) that can determine impurities present and the farther working distance is used for high resolution

images. Below is a comparison of the different graphite types from the closer working distance that can help determine the relative depth of field.

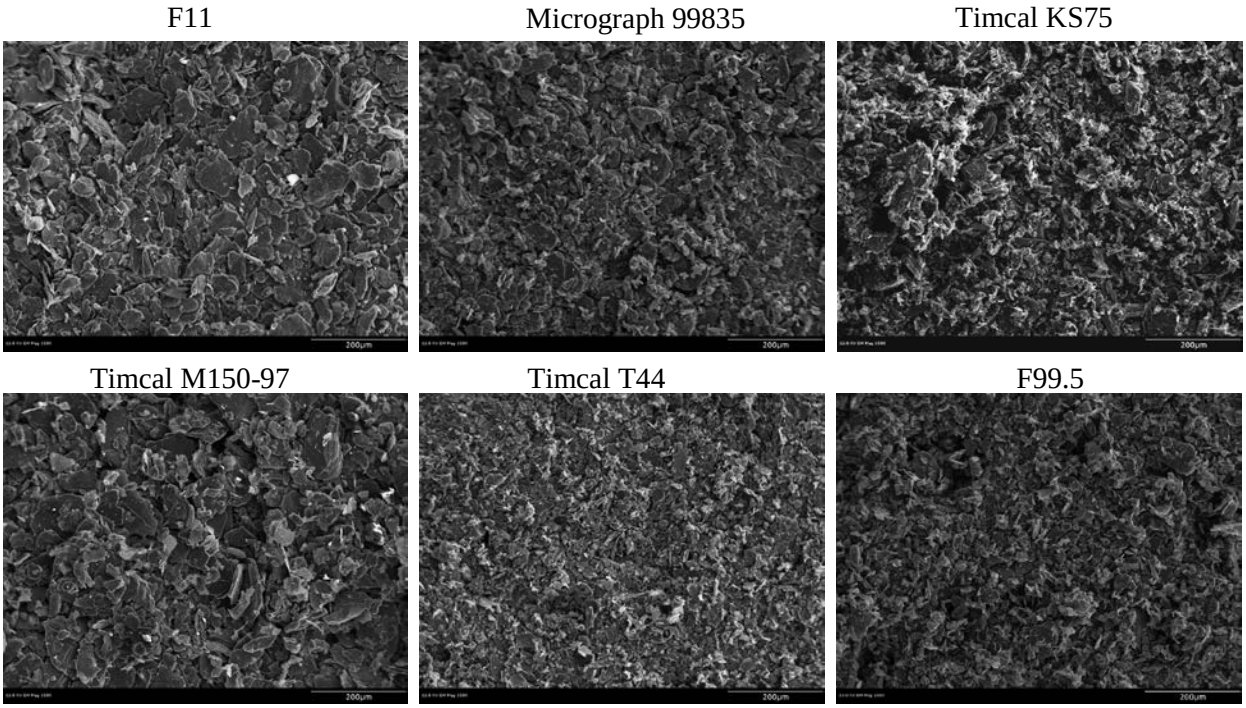

Figure 13: Comparison of Graphite Samples with a Working Distance of 13mm and Magnification of 100X.

There were major differences between the powders analyzed in particle morphology observed by using the SEM. The Timcal M150-97 and the Micrograph 99835 had a noticeable amount of fine particulate content. Timcal samples showed the most flake-like morphology while the F11 and F99.5 had somewhat more rounded features. The F11 and the Timcal M150-97 samples have large and round like flakes. The flakes can be visually seen with the F99.5, Micrograph 99835, and with the Timcal T44 as well but noticeably smaller than the F11 and the Timcal M150-97. The Timcal KS75 stands out from the other microstructures. There are some distinguishable flakes, but the orientation is random, making it appear that no ordered arrangement exists. The next set

of images are the same graphite samples, but the working distance has been moved farther back to 39mm, which gives these images greater resolution.

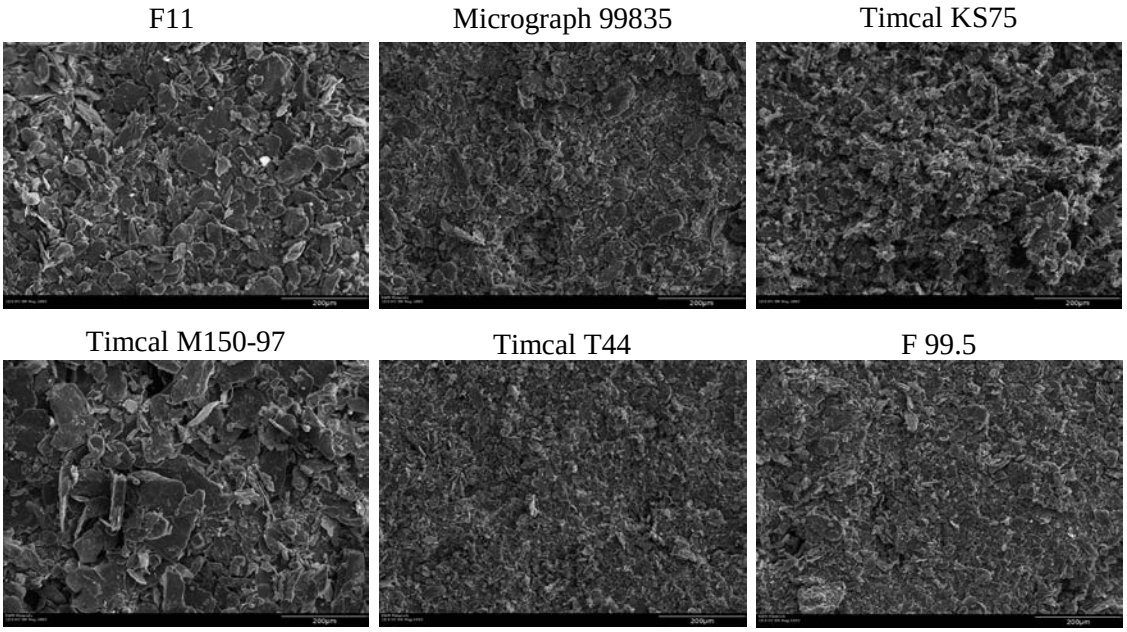

Figure 14: Comparison of Graphite Types with a Working Distance of 39mm and Magnification of 100X

These pictures show the structure of the graphite flakes and how tightly stacked on top of each other the layers are. The Micrograph 99835, Timcal T44 show smaller flakes and they're tightly packed with relation to one another. The F99.5 and Timcal KS75 have an intermediate flake size but different appearance. The Timcal KS75 seems to be quite porous whereas the F 99.5 is packed tightly together. Whereas the F11 and Timcal M150-97 have a larger grain size and the depth of the flakes can be seen along with some gaps between the flakes as well.

One of the special tools that can be utilized by a Scanning Electron Microscope (SEM) is the Energy Dispersive X-Ray Spectroscopy (EDX or EDS). It's an analytical technique used for the elemental analysis or chemical characterization of a sample and relies on interaction of X-ray excitation. The way each element is characterized is due to

its unique atomic structure allowing unique set of peaks on its X-ray spectrum. The energy of the X-rays is characteristic of the difference in energy between the two shells, and of the atomic structure of the element from which they were emitted; this allows the elemental composition of the specimen to be measured. Below are the EDX scans for each graphite sample that was being compared in this project.

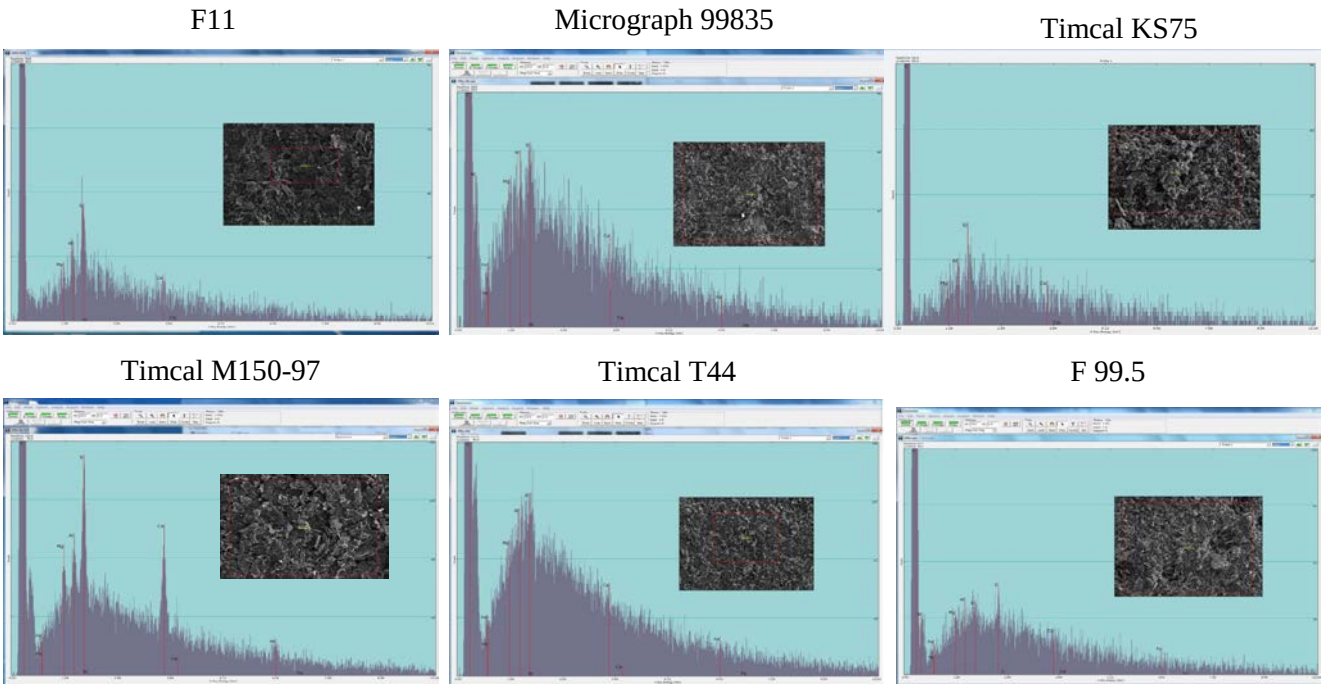

Figure 15: Comparison of all the EDX Scans at 100X

The scans might be difficult to look at together in this view, but there are some things that can be pointed out. Carbon is the predominant element present, and therefore its peak is the strongest by far. That's due to graphite being carbon, but other trace elements are present in varying amount for each sample. The smaller peaks come from other materials such as silicon, calcium, aluminum, magnesium, and iron. This is no surprise since graphite is naturally dug out of the ground using mining methods, making this material surround by these elements that are naturally found in the earth's crust in the form of oxides.

The specific results are hard to see with the sizing of the spectrums along with the elements that show up in the scan at this scale, and will briefly mention each material result. The table below gives a summary of the counts for each element present along with the time each sample was counted for.

Graphite Type	Mg(counts)	Al(counts)	Si(counts)	Ca(counts)	Time(sec)
F11	20	30	55	15	90
Micrograph 99835	40	48	50	25	60
Timcal KS75	10	15	25	10	90
Timcal M150-97	110	115	180	125	90
Timcal T44	100	124	140	70	90
F 99.5	32	40	45	20	60

Table 4: Counts for the Elements of Magnesium, Aluminum, Silicon, and Calcium

The results from this table clearly show the amount of relative impurities in each graphite sample. The reason the time varies between some of the samples were because the increase was done after the running of the Timcal KS75 and F 11 samples. The counts for Carbon are over 1,000 which should give some idea of the composition being predominantly graphite. Iron is not listed in this table because the results were very low in terms of count for some of the graphite samples. These results cover a very large area on the atomic scale with a magnification of only 100X and covering the highlighted rectangle as shown in the table. The counts were so low on these samples, that the time of the scan was increased from 60 to 90 seconds to produce a more accurate count. These two samples have a very low count of all the mineral elements meaning that they have a high purity. The counts were significantly lower on all the impurity groups as the table shows.

The two samples that have the shorter count time of 60 seconds can be grouped together as the medium grade purity samples. If we pro rate the counts to a 90 second window, the magnesium counts are approximately 50 to 60; aluminum and silicon are 60 to 75, and calcium is about 30 to 40 counts during that amount of time. The samples with the highest amount of impurities are the Timcal T44 and Timcal M150-97. It can be seen from the SEM images because there's a higher amount of contrast in those pictures and is likely due to the impurities that exist in the microstructure and the different elements radiate at different energy levels that caused the differing levels of intensity.

To characterize each raw material of graphite, a comprehensive summary of each material is put together containing images at magnifications of 100X, 200X, 500X, 1,000X with the working distances at both 13mm and 39mm. The EDX scan of each graphite sample is included in this section to summarize the results obtained from SEM of each material. The first sample to be looked at is the F11 and the first figure below is the images from the working distance of 13 mm.

100X

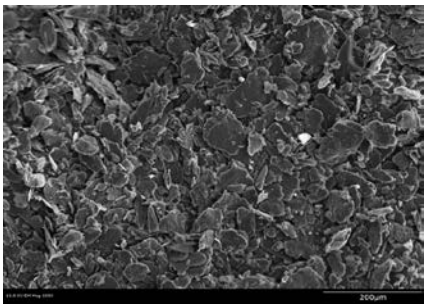

200X

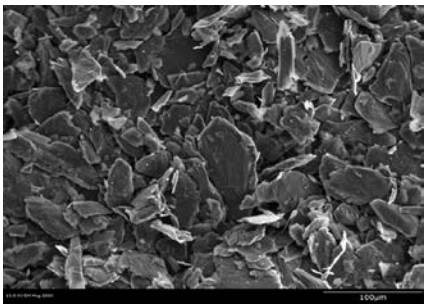

500X

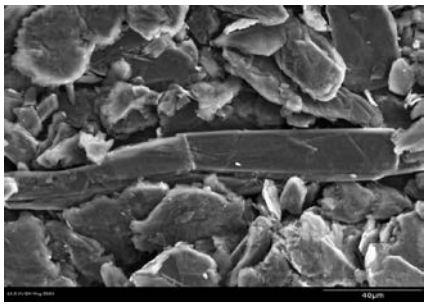

1000X

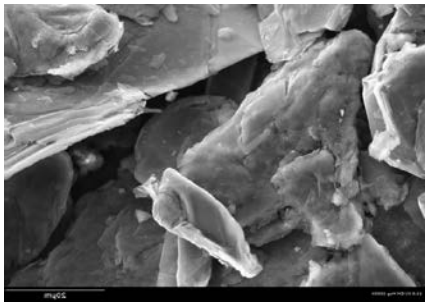

Figure 16: SEM Images of F11 Graphite at Various Magnifications at a Working Distance of 13mm

As the magnification increases, the arrangement of the flakes can be examined. The flakes tend to stack on top of each other and tend to be oriented in the same direction. The picture at 500X is quite unique with this large needle like flake going across the entire picture. Looking at the surrounding flakes, notice how they're all surrounding the needle one appearing almost only horizontal to the plane of the picture. The next image is the same sample but at the other working distance of 39mm.

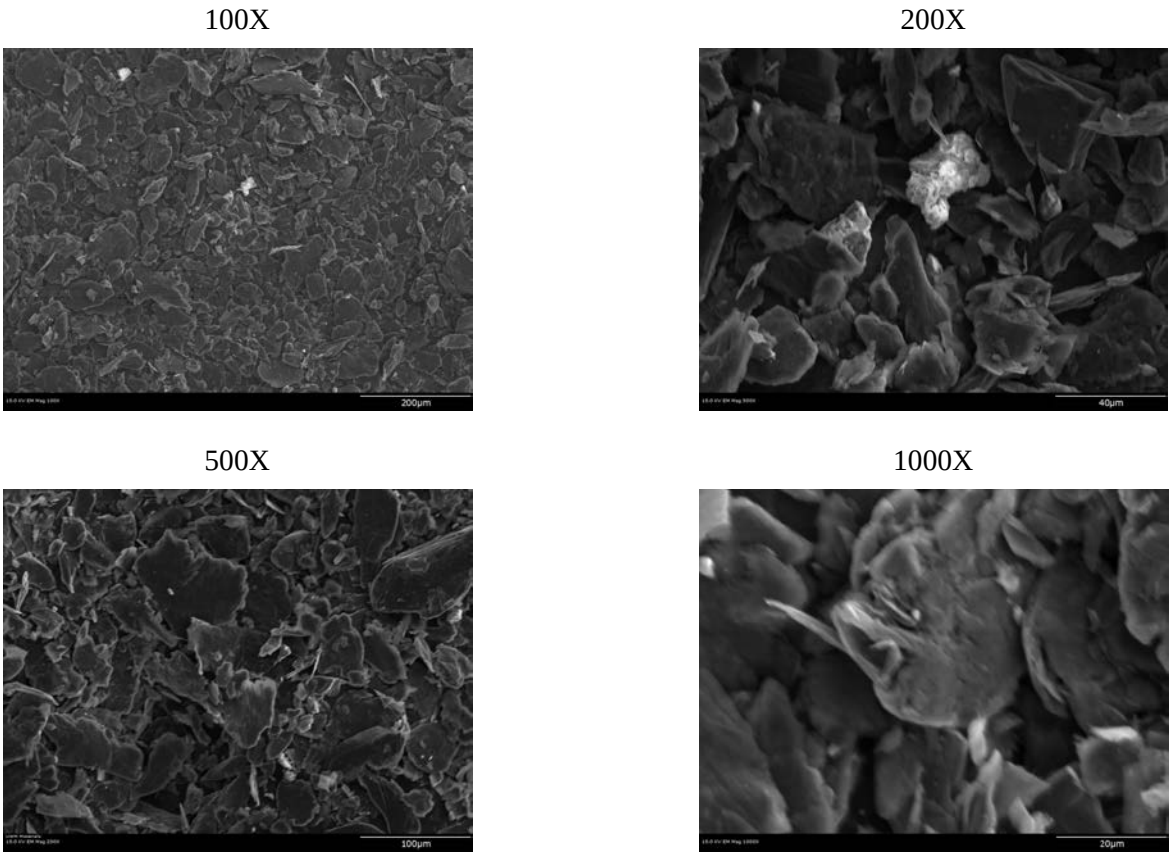

Figure 17: SEM Images of F11 Graphite at Various Magnifications at a Working Distance of 39mm

As the magnification increases on the F11 graphite, the proximity and orientation of the flakes stacked on top of each other can be observed. The packing stays close together as we increase the magnification of the F11 graphite. There seems to be a rounded shape to them as the focus shifts to the individual particles as the magnification increases. Finally, the EDX scan for the F11 sample determines the counts produced at different energies and gives an elemental analysis.

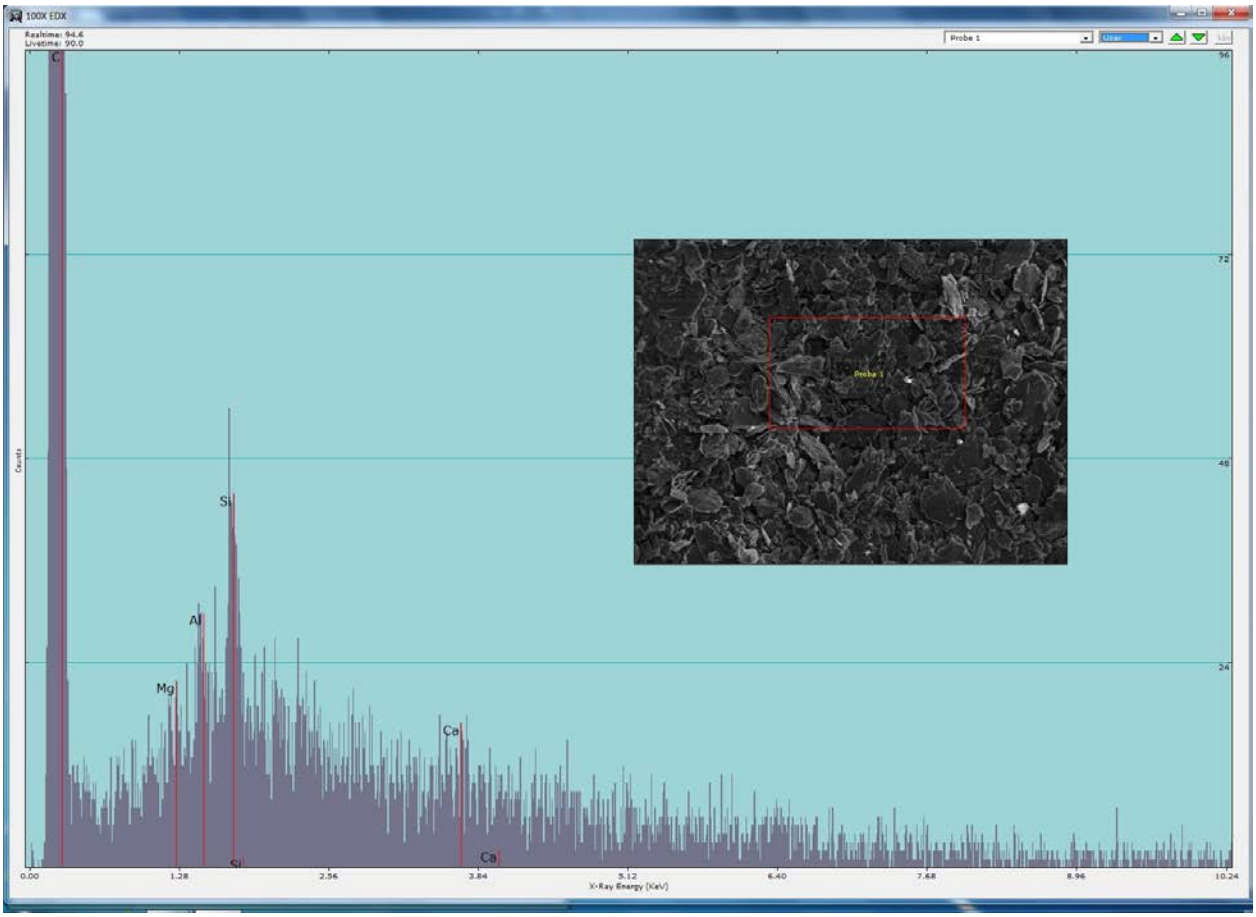

Figure 18: EDX Scan for F11 at 100X Magnification to Show the Overall Composition

Here's the result of the EDX scan for the F11 graphite sample. The red rectangle is the area that was scanned and the results are in the chart above. The focus here is on the elemental earth elements so carbon is cut out of the image to focus on the impurities. As mentioned earlier, F11 is a high grade purity compared to the other samples tested and therefore the peaks are lower than the other samples. The next sample that will be characterized will be the Micrograph 99835. The first figure below is SEM images that are taken from a short working distance.

100X

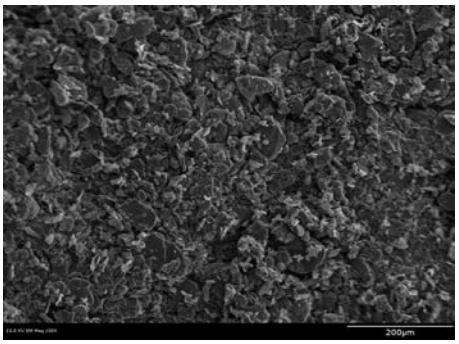

200X

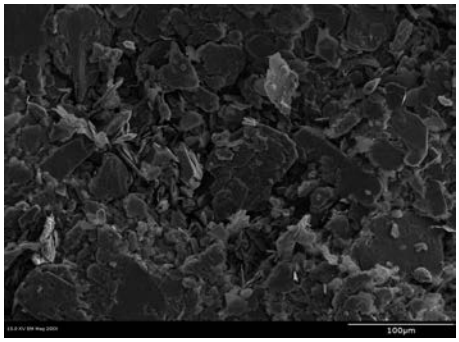

500X

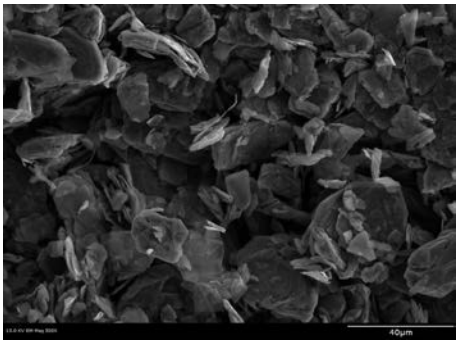

1000X

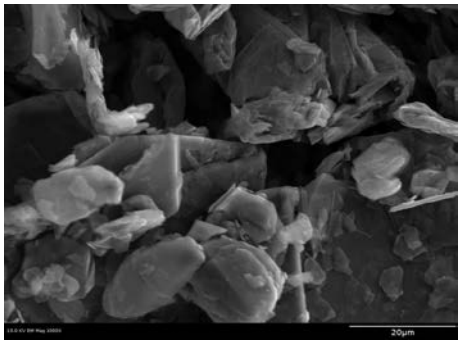

Figure 19: SEM Images of Micrograph 99835 Graphite at Various Magnifications at a Working Distance of 13mm

The microstructure for the Micrograph 99835 is shown above. At 100X magnification, it looks like there are a lot of small to medium sized flakes, but as magnification increases, the ability to focus in on some of the larger grains are possible. The size of the grains was larger than expected and there was more randomness in the orientation than expected. In the 500X and 1000X pictures, darker areas or holes between the flakes are quite noticeable. This explains why this graphite has a lower density than the other graphite samples.

100X

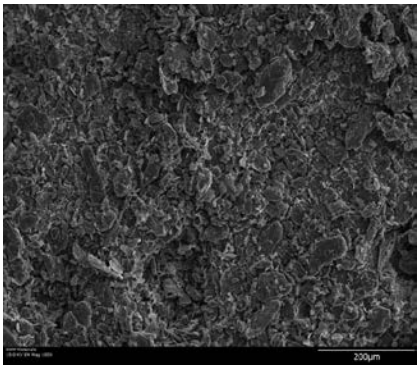

200X

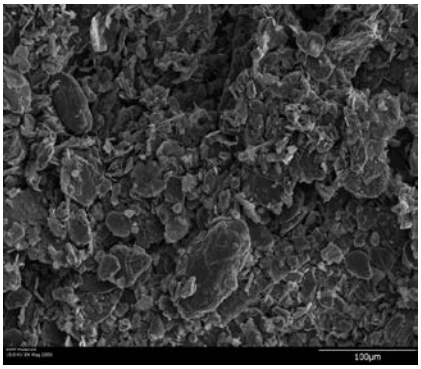

500X

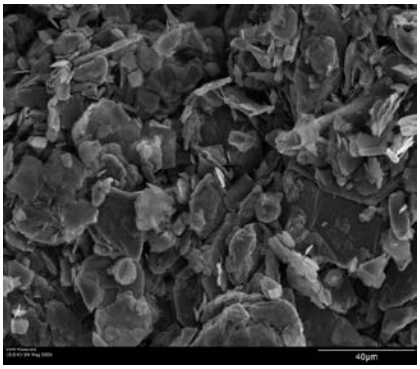

1000X

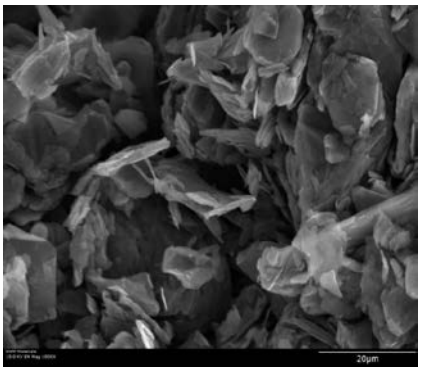

Figure 20: SEM Images of Micrograph 99835 Graphite at Various Magnifications at a Working Distance of 39mm

Here are the images taken at from 39mm giving us detailed resolution of the microstructure. The micrograph 99835 is a very fine structure. The individual flakes are small in diameter, but have a random orientation with creates small pores that are visible at 200x magnification. The size of the graphite particles seem to vary significantly which also contributes to the micropores.

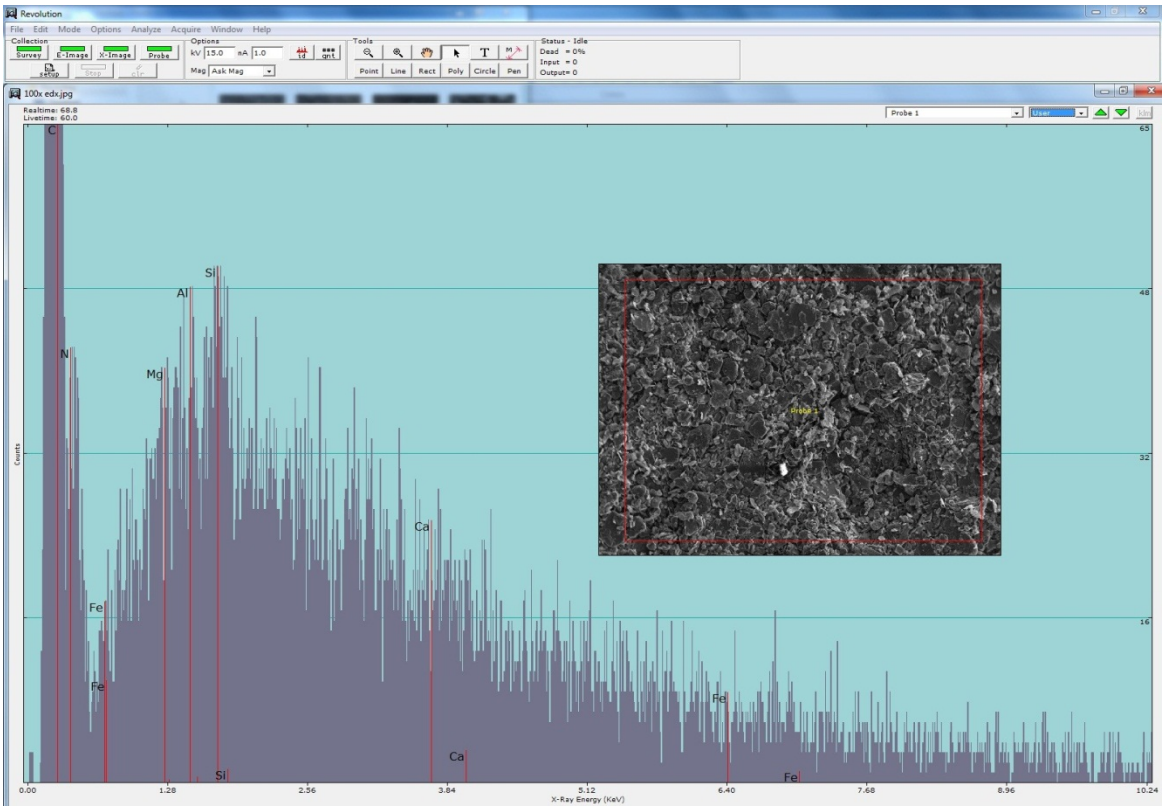

Figure 21: EDX Result of Micrograph 99835 Graphite at 100X

The results for the EDX scan for the Micrograph are shown in the figure above. The micrograph was found to be in the middle with regards to the counts of impurities as shown in the summary above. There is a distinct iron peak that can be made out from this spectrum. The count time is at 60 seconds instead of 90 which makes the results seem less than some of the other samples. The next material that will be summarized will be the Timcal KS75.

100X

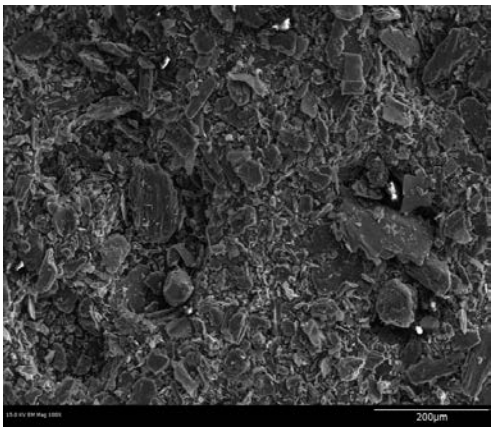

200X

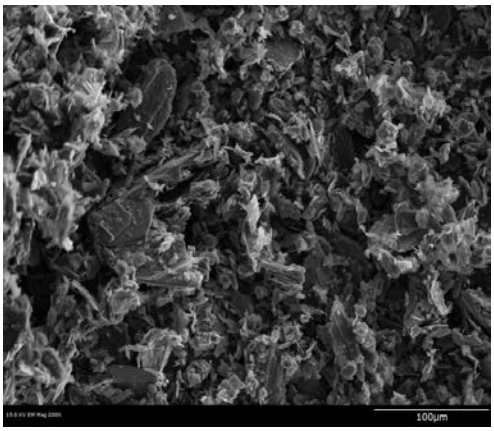

500X

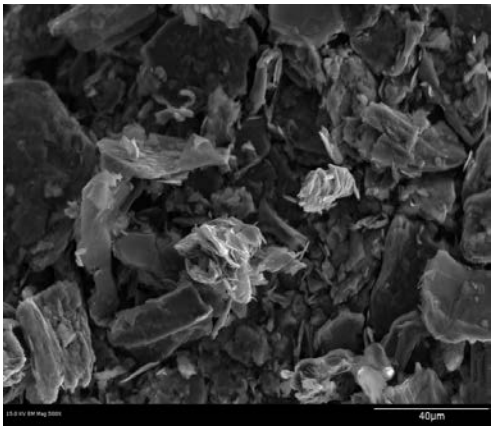

1000X

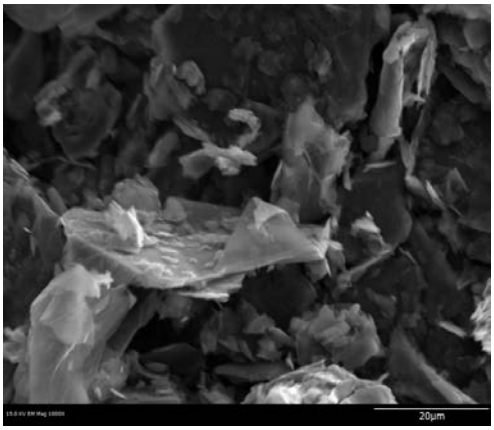

Figure 22: SEM Images of Timcal KS75 Graphite at Various Magnifications at a Working Distance of 13mm

As mentioned previously, the orientation with the flakes have a more random orientation than the other graphite samples. As the magnification increases, it becomes easier to see the way that the flakes orient themselves with respect to each other. There aren't as many holes that can be visibly seen considering the orientation and the density of the Timcal KS75 is higher than some of the other graphite samples. Next are some more images of this material from a farther distance for some better resolution.

100X

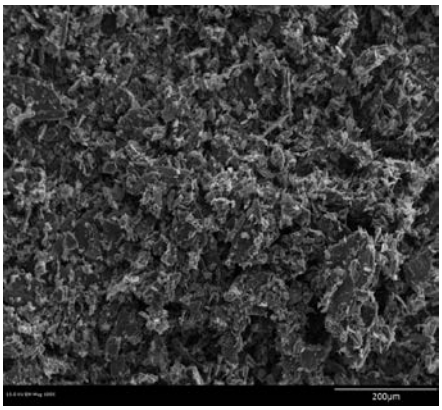

200X

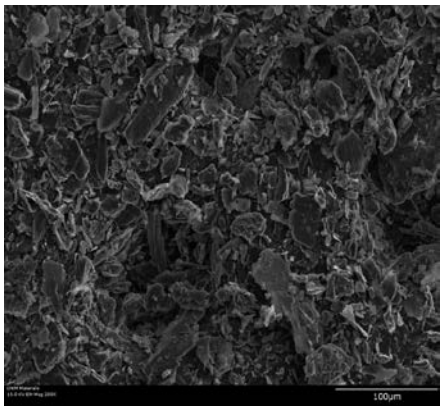

500X

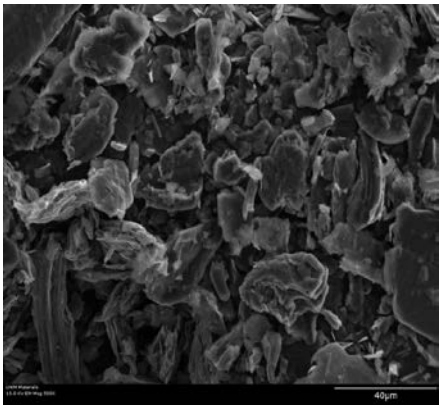

1000X

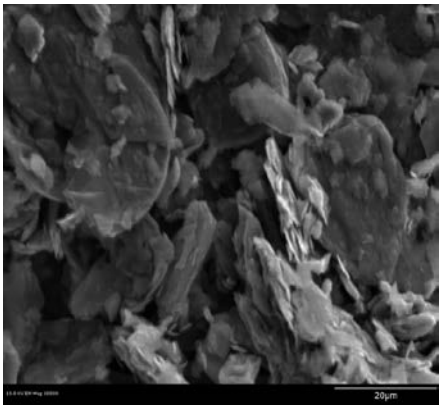

Figure 23: SEM Images of Timcal KS75 Graphite at Various Magnifications at a Working Distance of 39mm

The Timcal KS75 graphite has a smaller flake size. The orientation seems more ordered than the other graphite materials causing very few micropores within the structure. As the magnification increases, it can be seen that the flakes have the same orientation which would also explain the close packed structure. The next figure below will be the results from the EDX scan.

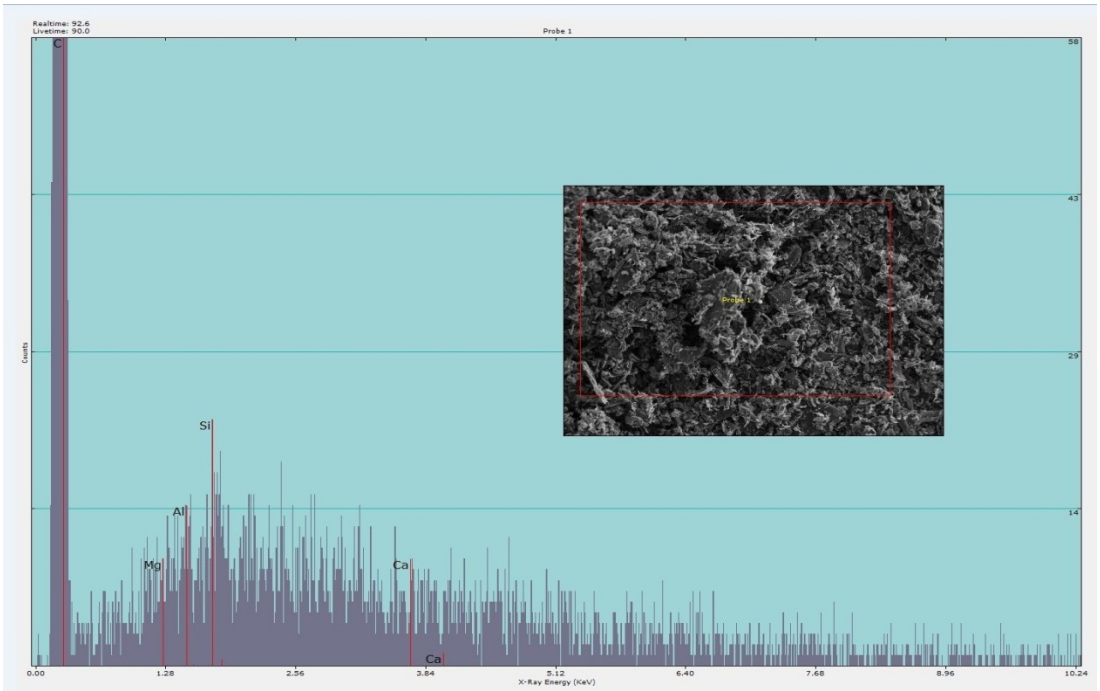

Figure 24: EDX Result of Timcal KS75 Graphite at 100X

Here is the EDX spectrum that was recorded for the Timcal KS75. As the table presented, this material has a high level of purity and has very little impurities present. This material had the fewest amount of impurities out of all the types of graphite that were tested. Timcal M150-97 is the next graphite sample that was examined.

100X

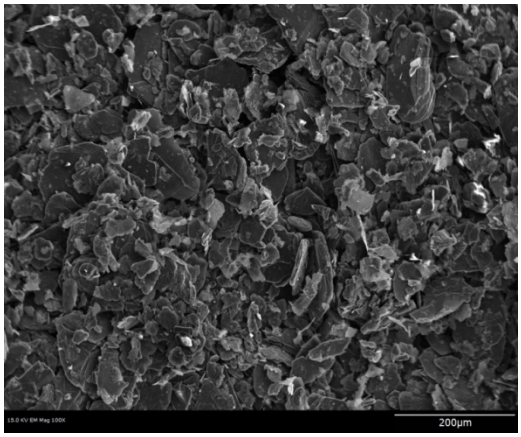

200X

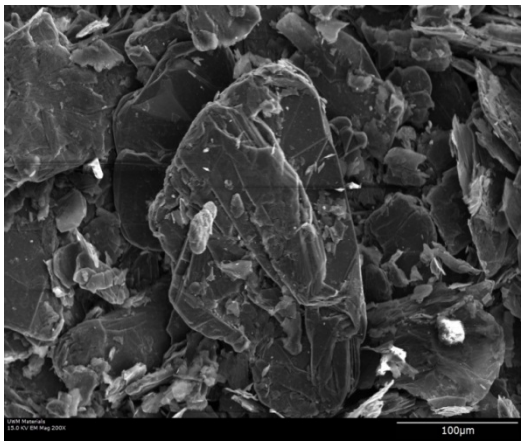

500X

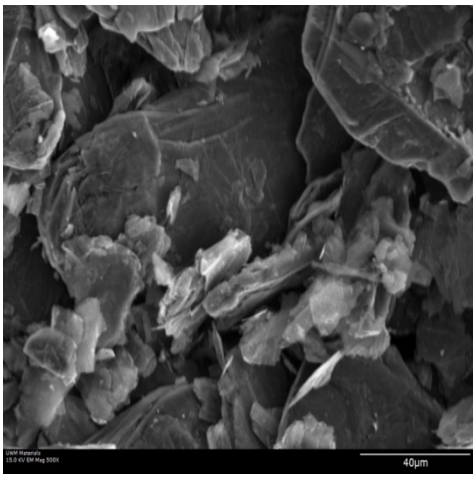

1000X

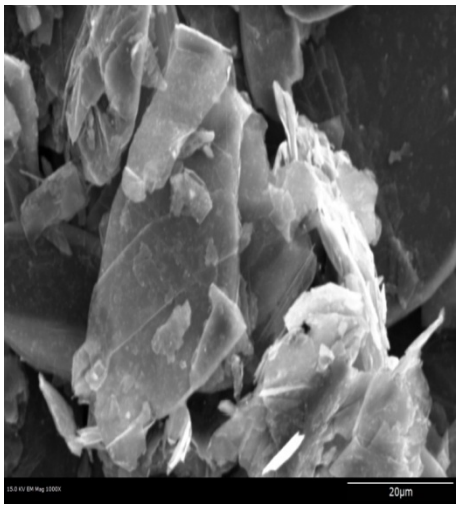

Figure 25: SEM Images of Timcal M150-97 Graphite at Various Magnifications at a Working Distance of 13mm

From the pictures shown, the relatively large flake structure and how they stack on top of each other stand out in the image above. What looks unique about the Timcal M150-97 is the varying flake size that forms. There are large flakes that tend to orient themselves in a similar way to each other and the smaller flakes that stick out between the larger ones creating a compact structure. This material has the largest range of flake size of any of the graphite samples.

100X

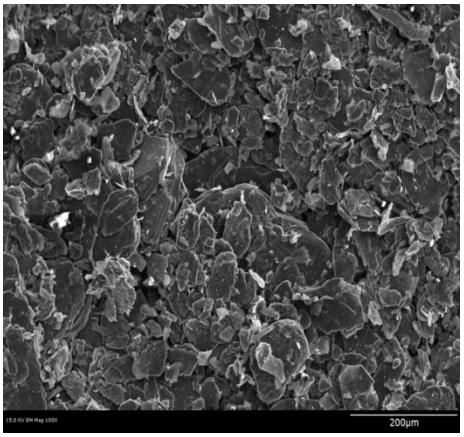

200X

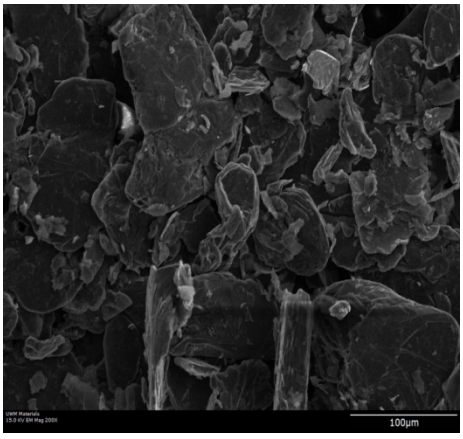

500X

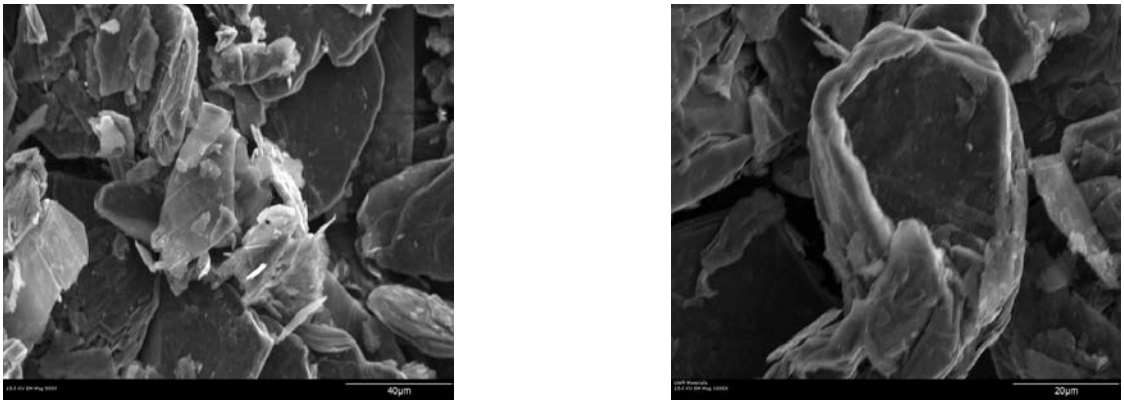

Figure 26: SEM Images of Timcal M150-97 Graphite at Various Magnifications at a Working Distance of 39mm

For the Timcal M150-97, the large flake size and the large pores within the structure is clearly visible. The shape of these flakes has an oval shape to them. Looking closely at the 100X, there are a couple very bright areas and is due to the overall shiny appearance to some of the flakes and from the evidence provided from the EDX results, shows that this is from the impurities present in the material itself. The next figure is the EDX scan from the Timcal M150-97.

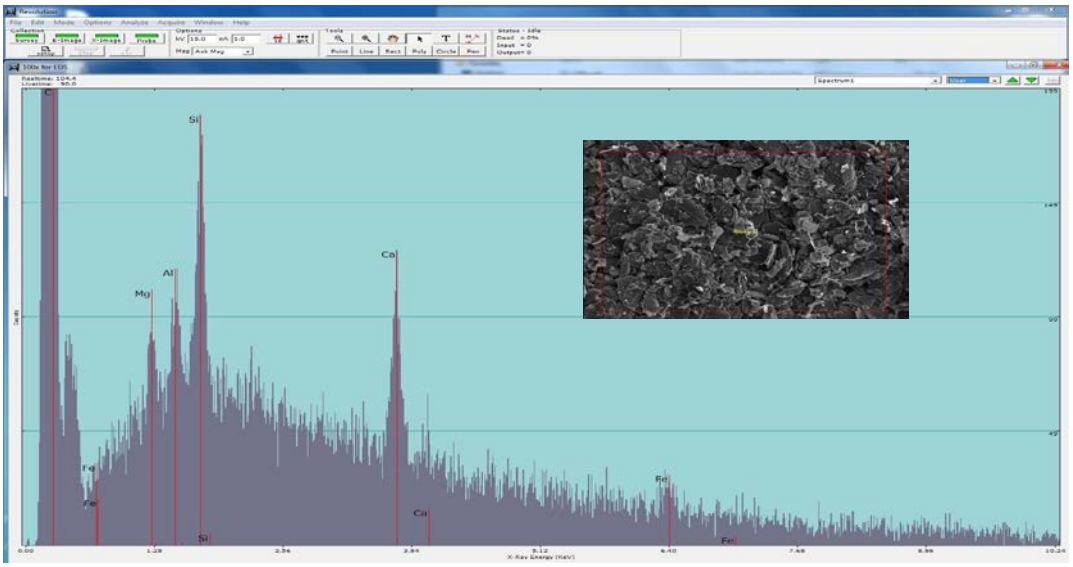

Figure 27: EDX Scan of Timcal M150-97 Graphite at 100X Magnification

As mentioned earlier in the images, Timcal M150-97 has the highest counts of impurities out of all the graphite samples tested. All the different impurities are distinct in this spectrum, including iron which was indistinguishable in some of the scans. The picture in the scan above shows the area that the scan took place. The shiny areas are from the impurities in the sample since graphite shows up pretty dark since it doesn't send off a strong reflection from the electrons. The counts for all the major impurities are all over 100 and are considerably higher than the other materials and create this shiny residue on anything this material touches. The next material that will be characterized will be the Timcal T44.

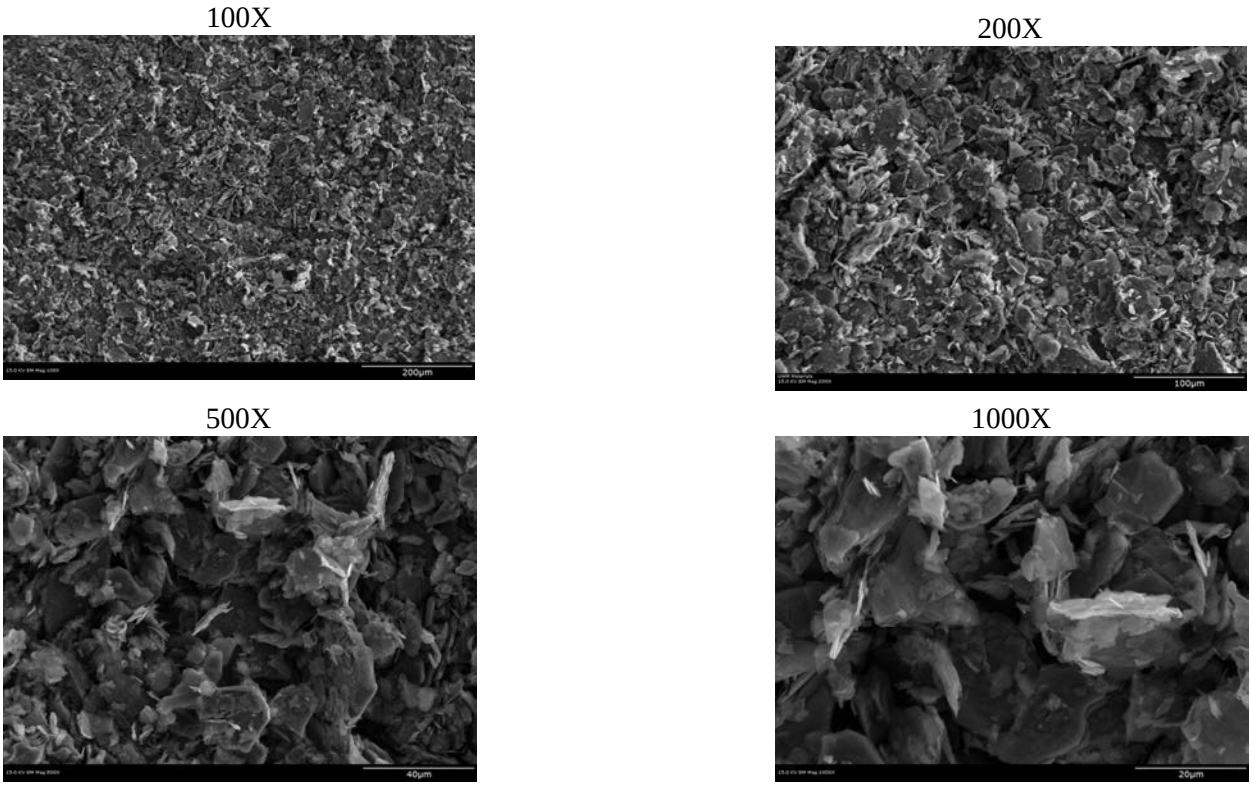

Figure 28: SEM Images of Timcal T44 Graphite at Various Magnifications at a Working Distance of 13mm

From the pictures taken using the SEM, there's a clear resolution that this material is composed of many small flakes. This creates a compact microstructure with very few pores. The EDX results show that the T44 has a high number of impurities and the contrast level would lead to that premonition as well. When the magnification is increased to 500X and 1000X, the orientation of the smaller flakes with respect to each other are clearly visible. The orientation of the flakes appearance becomes more random and tiny holes within the structure can be seen. The next series of images are from a farther working distance of the Timcal T44.

100X

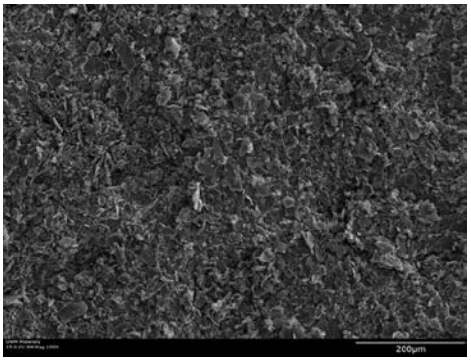

200X

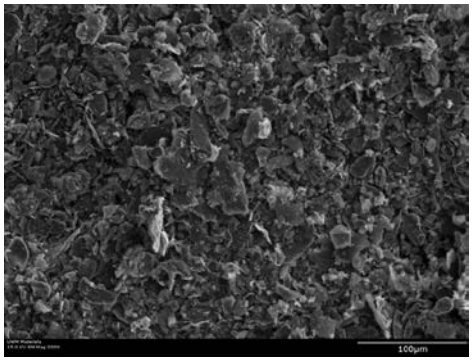

500X

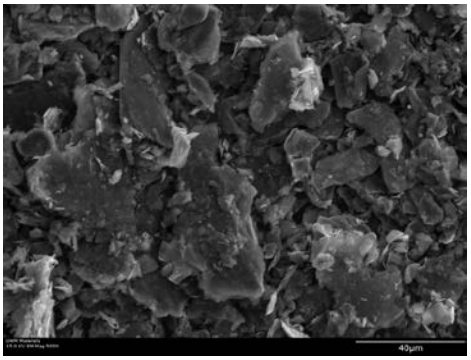

1000X

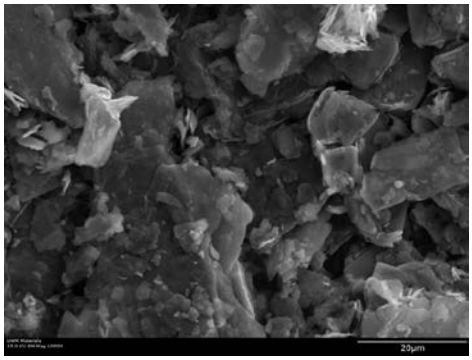

Figure 29: SEM Images of Timcal T44 Graphite at Various Magnifications at a Working Distance of 39mm

The different graphite particles from the Timcal T44 are very small in size and oriented in such a way that there aren't any significant pores within the structure. The

higher magnifications show how the different orientations fit closely together having a smaller number and size of pores. The shape of these flakes appears to be more needle like, whereas some of the other samples have a circular type of structure. The image at 200X shows a larger sized impurity with the bright intensity in the lower left hand corner. Finally, here is the EDX scan for this material.

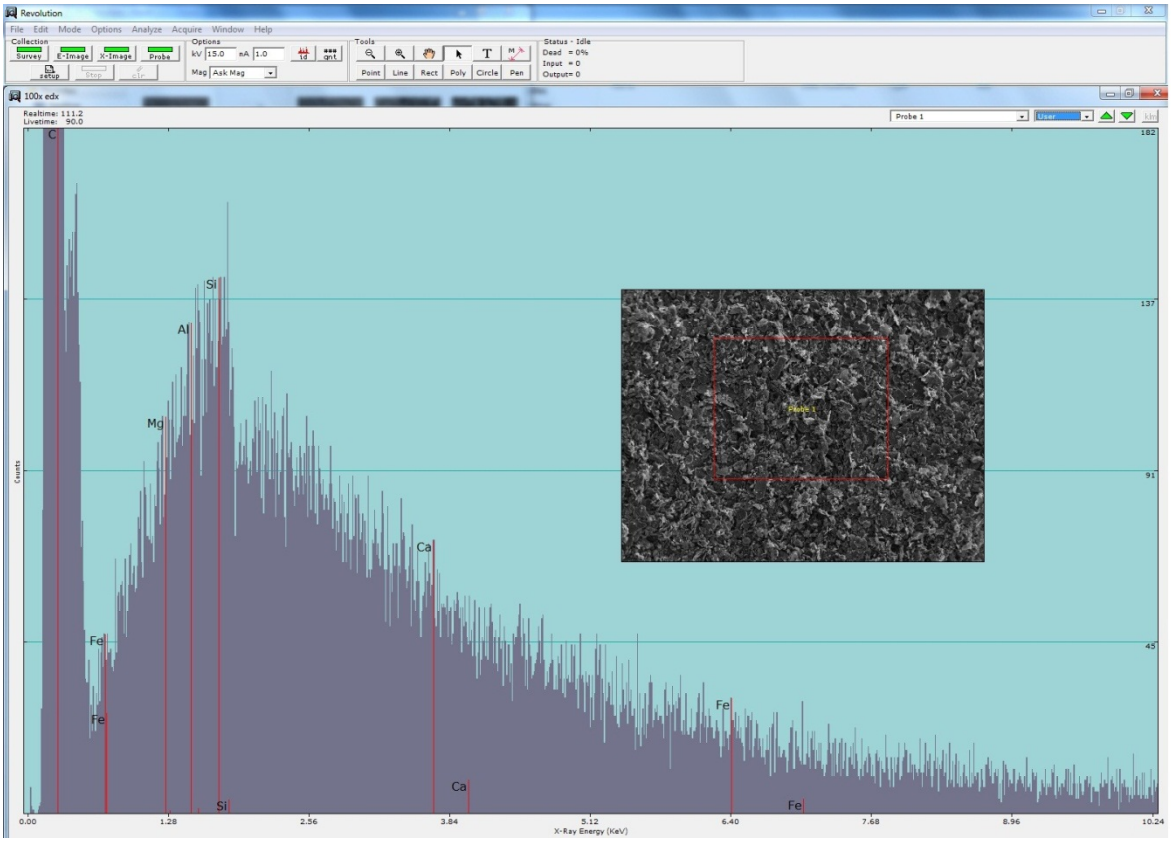

Figure 30: EDX Scan of Timcal T44 Graphite at 100X Magnification

The EDX results for the Timcal T44 are presented in the figure above. This has a high impurity count, with magnesium, calcium, and silicon all over 100, while the calcium is at approximately 75. The only sample with higher impurity counts is the Timcal M150-97. Both peaks for iron are visible in this spectrum and labeled in the figure above. Now it's time to examine the final material being characterized, the F99.5 sample.

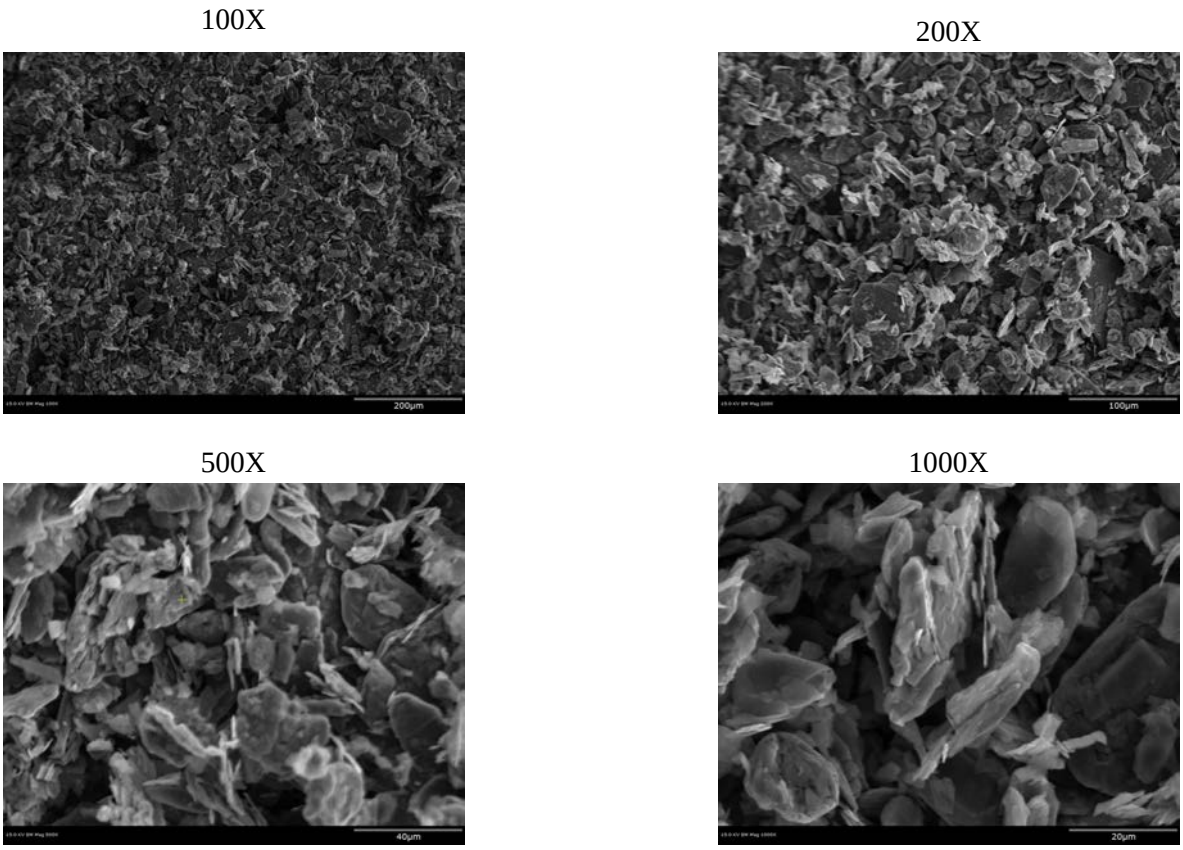

Figure 31: SEM Images of F99.5 Graphite at Various Magnifications at a Working Distance of 13mm

Finally, there's the F99.5 material that is composed of primarily smaller flakes with some larger ones within the structure. This material looks fairly porous in the pictures taken, so this could be a good candidate to insert copper into. The orientation looks quite randomized as well when looking at the sample at higher magnifications. At 1000X, the different elevations of the graphite at the surface of the material can be clearly seen by the different areas of contrast. There are a few grains in the center that stand out while the surrounding area is dark and unoccupied.

100X

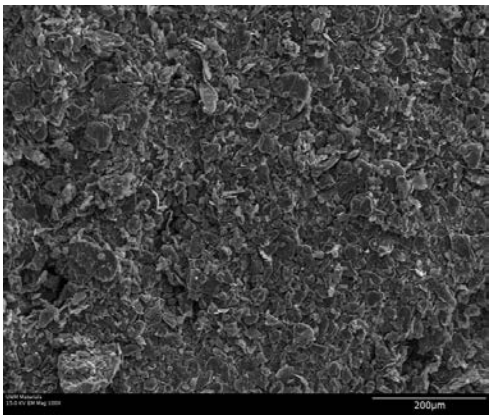

200X

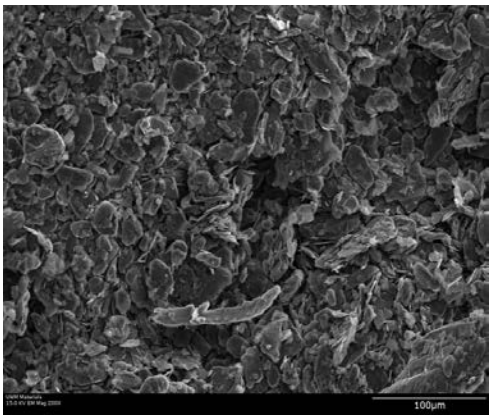

500X

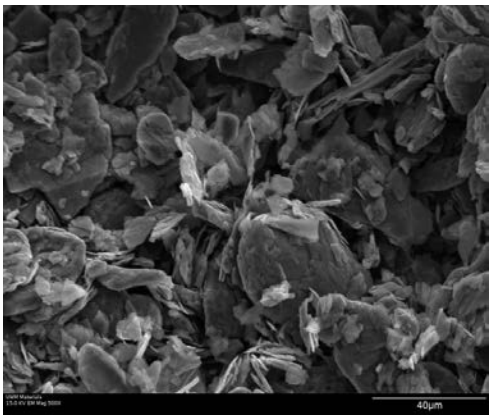

1000X

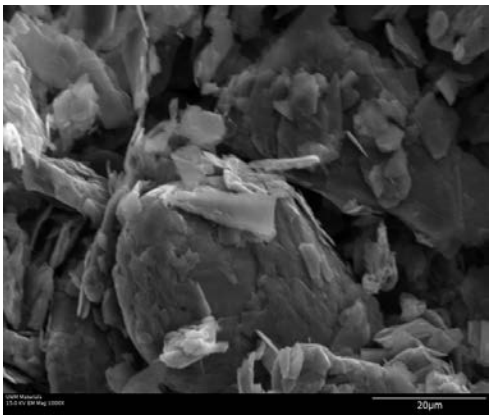

Figure 32: SEM Images of F99.5 Graphite at Various Magnifications at a Working Distance of 39mm

The F 99.5 appears to have a closely packed structure along with a small particle size. As magnification is increased, some pores between some of the flakes become visible. The shape of the flakes varies considerably with some being quasi-circular and there are some needlelike ones as well. At higher magnifications, the flakes are randomly oriented in a way that makes the structure closely packed together with very few micropores.

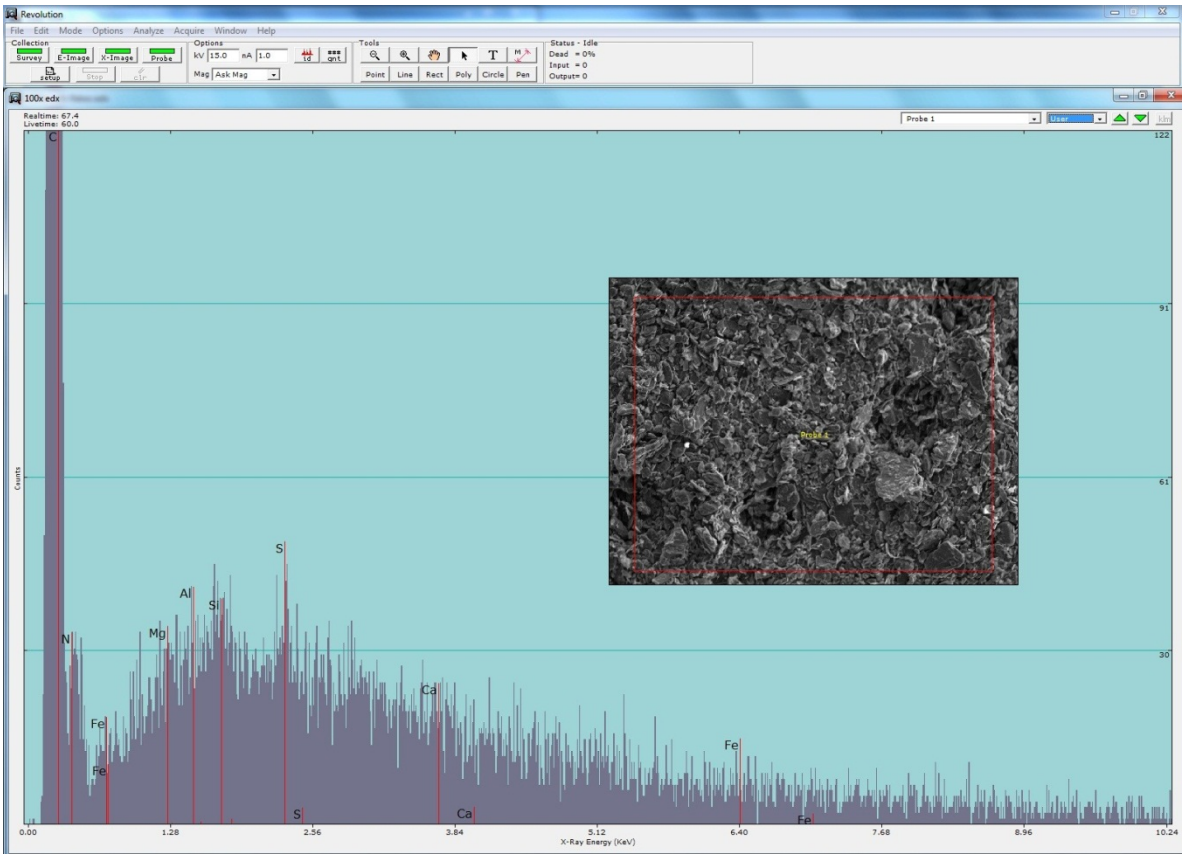

Figure 33: EDX Spectrum of F99.5 Graphite at 100X Magnification

Above is the resulting EDX scan of the F99.5 graphite. What is unique about this result is the apparent presence of sulfur. It is quite significant and seems to have the highest impurity count over magnesium, aluminum, and silicon among others. More work needs to be done to determine in what form the sulfur exists within this material.

This concludes the SEM results and is the primary source of characterizing the six types of graphite being examined. The Timcal KS75 and F11 have higher grade of purity and that is reflected by the EDX results along with the images taken with the SEM due to the lack on contrast. On the other hand, the Timcal T44 and Timcal M150-97 have sharp contrast in the SEM images and correlates well with the level of impurities.

EXPERIMENTAL DIFFICULTIES

Characterizing the raw materials was the first step in this process and obtaining results were straight forward, but that wasn't the case for samples that went through the first step of the intercalation process. There were severe issues related to getting $CuCl_2$ intercalated. The main issues related to accomplishing this are: ampoules imploding in the furnace, opening the ampoules if they survived the heating and recovering the intercalated material after opening the ampoules.

After adding the graphite and $CuCl_2$, the samples were then taken to the glass shop to get vacuum sealed so that the material was not exposed to atmospheric conditions. This was done to prevent moisture in the air to affect the materials in the ampoule, especially the anhydrous $CuCl_2$, since it readily reacts with H_2O along with the lowering of the internal pressure of the ampoules. As seen in figure 34 below, this does not prevent the ampoules from being unrecoverable. The samples imploded from the pressure caused from heating the samples to higher temperatures.

Figure 34: Results from a preliminary trial to intercalate $CuCl_2$ into graphite

The ampoules like imploded as opposed to exploded during heat treatment. Looking along the right hand side of the image in Figure 34, it is apparent that the ceramic hearth broke into several pieces. That is used as a spacer to help provide even heating to the objects placed on it. There is also a considerable amount of discoloration within the furnace due to the graphite being expelled from the imploded ampoule. The powder is light and free flowing, making the remnants hard to contain.

After reviewing the current procedure, there were a couple factors that needed to be investigated further. The factors that needed to be reconsidered were the amount of

material put in the sample, and the configuration of the ampoule itself. Both of these considerations are related to reducing the initial amount of internal pressure contained in the ampoule.

The initial dimensions of the ampoule were 25mm diameter with a height of 9mm and the top part had a diameter of 11mm and was designed for easy vacuum sealing. Vacuum sealing was an issue and was able to lower the internal pressure to only 100 millitor. This was with the weight inside the sample containing 15 grams of material. There was no previous method that used this amount of material within an ampoule. The reason this was attempted was due to making enough final material that enough material would be produced for the whole procedure, including analysis. The first adjustment that was made was lowering the material inside the sample from 15 grams down to 7 grams. This is the quickest and easiest step to lower the internal pressure within the ampoule, but this didn't prevent the ampoules from imploding. The image below is what an empty ampoule looks like and even though the dimensions changed during research, the overall shape remained the same.

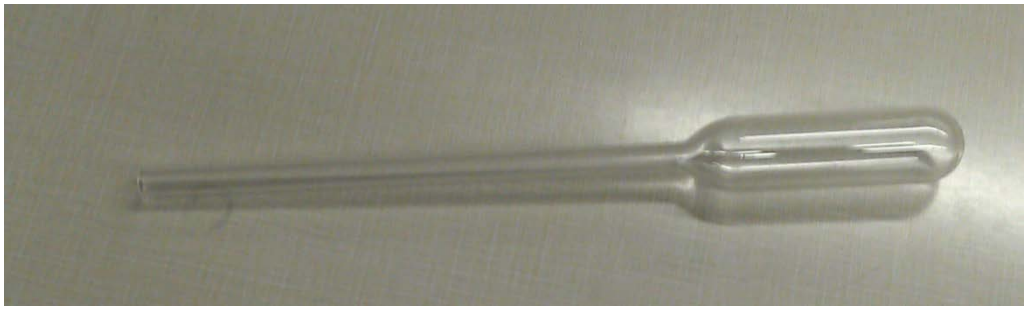

Figure 35: An Empty Ampoule with dimension 22mm outer diameter and 7mm length at the bottom with 19mm outer diameter at the top with thick wall tubing glass.

The next step was to change the dimensions of the ampoule so that there was less empty space inside of it and that improve the vacuum seal on the ampoule. The

dimensions were reduced to a diameter of 22mm with a length of 7mm, and the top portion had a diameter of 9mm. The wall thickness of the tubing changed as well from medium wall tubing to thick wall tubing to make the ampoules safer during the intercalation process. Pictured above is and empty ampoule with all the modifications previously mentioned. These changes lowered the overall volume significantly, but this didn't significantly improve the overall performance of the ampoule. The internal pressure after all of these changes decreased, but not drastically with the internal pressure still residing at 60 millitor.

Some of the ampoules put into the furnace didn't implode during the heating process. Although, trying to open the ampoules safely and easily was difficult because of the internal pressure within them. After consulting with the person who helped design and build the ampoules in the glass shop, the best approach to open them was by striking the tip where they were sealed with a hammer. Using the hammer to strike the tip created issues with safely opening the ampoule and collecting intercalated material for analysis and for the chlorine reduction step. Pictured below is what a sealed ampoule looked like after it survived the intercalation process.

Figure 36: Sealed Ampoule after Step 1 of Intercalation

The initial plan was to wrap the ampoule in a cloth and paper towel to contain the glass and powder and was thought to be sufficient. The energy released during the

implosion was significantly larger than anticipated and forced additional precautions to be considered. When striking the ampoule with the hammer, it wouldn't always break on contact making the environment less predictable. The sealed end of the ampoule where the powders were put in from was the area where the seal would be the weakest. When attempting to break the ampoule, parts of the sealed ampoule would chip off into small pieces but the seal remained intact, making the targeted area smaller and harder to open. When the ampoule finally broke, a loud booming noise would follow along with a small cloud of powder resonating in the vicinity of where it was broken.

The initial plan results expected to be that the cloth would absorb some of the energy from the implosion, but the force would be great enough that the multiple layers of cloth would rip and unravel itself in the process. The first sample, the ampoule was held in the left hand while trying to break the ampoule with the right hand; the ampoule disintegrated upon rupture. After that, it was necessary not to suspend the ampoule in the air by holding it with the left hand and thus it was laid atop a counter to help balance and anchor the ampoule along with absorbing some of its energy. With all those precautions in place, it still was not safe enough.

There was one incident during this project that resulted in an injury. When trying to open an ampoule, the force was so significant that it ripped through the cloth, through the lab gloves, and broke through the skin of the hand. There were several small lacerations with shrapnel all over the left hand glove and on the hand where the glove failed. Thankfully, there were no serious injuries and after a brief trip to the campus medical center. After that incident, it was determined that the procedure of how to open the ampoule safely needed to be adjusted.

The initial attempt to break the ampoule was to use a glass cutter to score the glass and create an area on the neck where the ampoule would break cleanly. That idea did not work so well because it was very hard to scratch the glass all the way around the neck in the same groove. The glass cutter would get caught up on the neck and the narrow area by the seal wasn't long enough to get the proper clearance to induce breaking at that spot effectively. The overall result was no significant improvement, and the blades for the cutter wore out very quickly in the process. After this failed attempted the consensus was that the ampoule had to break in an enclosed area to prevent another incident from happening again. Dr. Church came up with the idea of using a door hinge like apparatus in a plastic container filled with insulation to encapsulate the implosion. Below is what the apparatus looked like from several different viewpoints.

Figure 37: The Door Hinge Apparatus Used to Make Ampoule Breaking Safe

This device was created by Dr. Church and by looking at the picture on the left shows what the ampoule breaker looks like on the inside. The breaker is entirely enclosed within a plastic container that's surrounded by foam. This was done to completely enclose the ampoule as its being broken and to prevent any further injury. The middle picture shows where the ampoule is inserted into, and to be able to insert the ampoule, the door hinge must be flat across so that it can be broken along the neck. Finally, the image on the right shows how to break the ampoule. There was a hole drilled into the lid of the

plastic container to ensure that no debris or material escape the ampoule breaker. A screwdriver is inserted into this hole to push the door hinge until the ampoule breaks and the resulting material can be collected. There were some complications to this method in accumulated the intercalated material though.

The final issue encountered was how to accumulate and extract the intercalated powder after the implosion. The first couple times after breaking the ampoule, it wasn't possible to accumulate the powder to process it any further. When holding the ampoule by hand, the powder fell to the ground. After laying the ampoule atop of a counter, the powder and the glass ampoule intermingled and the two materials had to be separated. The process started by removing the larger pieces of glass and was done very carefully by hand. Problems came through this step because there were two different stages present in the ampoule during this stage. There were both intercalated graphite and excess $CuCl_2$ present, but most of the excess copper chloride stayed attached to the ampoule itself. Then to remove the excess $CuCl_2$ ions, a vacuum pump was used to filter out the diluted HCl solution and the excess chlorine atoms from the intercalated powder.

To end with up with solely the intercalated graphite, the remaining material was dried in the vacuum oven at 60^oC for 12 hours. The time and temperature were picked in such a way that the water used to wash the sample after the filtration process would evaporate without the material reacting with the atmosphere. The issue related to this was that the end product was a very miniscule amount and this made the amount from a single ampoule impossible to analyze. To do the characterization of this intercalated material as done with the raw materials of graphite, we need approximately three to five grams for all the tests. The result from an ampoule that had seven grams of material put inside of it and

then sealed yielded well under one gram of product.

Considering the stability of the ampoules in the furnace and the time it takes to process them, the timeframe to accomplish reproducible results took a significant amount of time. Three ampoules were processed at once, but either all or none of them would survive the heating process, and usually the ampoules would implode. These are the reasons why this project was a major challenge in coming up with measurable results. Both the technique and process need to be refined and mastered before reproducible results can be achieved.

CONCLUSION: FUTURE WORK

There is still more work to be done before this project is completed. Before any comparable results can be obtained, the process must first be mastered. Once that has been resolved, the intercalated material needs to be analyzed to see how much $CuCl_2$ has entered the graphite structure and the stage of the graphite intercalated compound needs to be examined. Next, the chlorine reduction step would strip away the chlorine atoms that are still attached to the copper within the structure, and finally final material could be analyzed to characterize the overall composition of the copper intercalation within the graphite and the performance of the material compared to raw graphite.

The issues that have prevented this project from delivering measurable results relate to the stability and overall result from the material in the ampoules. Optimizing the conditions to prevent the ampoules from imploding in the furnace during the intercalation process is necessary to progress in this project. The issues that need to be overcome with respect to the ampoules are as follows: 1) Can a lower furnace temperature create favorable conditions for intercalation, 2) Find a better way to execute the ampoule filling process, and 3) Find a better location to store the materials.

Looking further into possible solutions to the issues, lowering the furnace temperature to find out if the ampoules are more stable would be the easiest adjustment to make since it does not change the procedure or any other parameter and should lower the internal pressure on the ampoules. The next possible solution would be to store all the necessary chemicals in a glove box to prevent moisture from accumulating in the ampoules and chemicals, especially Copper (II) Chloride. As the stability of the ampoules increase and the method is mastered, research would pick up with the focus switching to

characterizing the amount and stage of intercalation that takes place. This would include the same evaluation that took place with the raw graphite material and would include SEM, BET, XRD, and TGA.

There are also some issues related to XRD that need to be addressed. In the preliminary characterization, there were not any peaks that could be characterized from the impurities. There are approximately five areas of interest that are worth investigating into further. To do so, it would involve increasing the current of the machine to intensify the peaks and the counts during the scan. The other adjustment that would be necessary would be to slow down the scanning rate to develop a more accurate and detailed scan to help refine the preliminary results. The way to work around this issue would be to run the XRD scan under the same conditions as the initial characterization process and analyze the difference in the two patterns. The same process would be done with TGA and BET to determine the relative amount of intercalation that took place within the ampoule. The other major characterization taking place during this step is using the EDX feature of the SEM to approximate the overall composition of the intercalated material, especially with regards to the copper and chlorine content within the structure.

The other way research would pick up would be initializing the second step of this process, reducing the chlorine in the graphite intercalation compound. There is a significant amount of setup in this process. The idea behind the chlorine reduction process would be to have Ar 4% H_2 gas flowing through a quartz tube that would be sealed at both ends so the intercalated graphite would not be exposed to any other elements. The quartz tube is enclosed and surrounded by a furnace with the graphite being with the quartz tube. On the other end of the tube where gas is flowing in, there

would be a tube that leads into a container of water. The reason that the gas exiting the quartz tube is going into a container of water is due to safety issues. The chemical reaction below is the net equation taking place in the quartz tube furnace:

$$H_2\ (v) + CuCl_2(s) = 2HCl\ (v) + Cu(s)$$

As the equation shows, this produces a volatile vapor of hydrochloric acid. The options to accomplish this would be to operate this step under a fume hood to evacuate the odor associated with this reaction or run the tube into a beaker of water so that there would a diluted solution of hydrochloric acid that would be disposed of properly in a safe and effective manner. This step could be optimized and adjusted after running the same conditions with the TGA by studying the weight change kinetics under the same conditions the graphite undergoes in the furnace and quartz tube apparatus.

Once the process has been optimized and samples have gone through the chlorine reduction stage, the last step is the final characterization. Along with the SEM, TGA, XRD, and BET that has been done in every stage there are a few new analytical techniques that are suggested. One of the major unknowns of this project is the intercalated material's resistance to oxidation, especially with regards to thermal stability. The desired application for this material will expose the material within the electric brush to high temperatures that could lead to some oxidation and quick decomposition. Another aspect that needs to be investigated is the mechanical properties of the intercalated material. For this test, it would require a nanoindenter. This procedure and method has become very popular over the last couple of decades since it only requires a small amount of material for the test and it is ideal for powders [15, 16].

Another important test that is important for this application is pin-on-disc wear

testing. Another word for an instrument that does this kind of testing is a tribometer. Pin-on-disc consists of a stationary pin under an applied load in contact with a rotating disc. The pin can have any shape to simulate a specific contact, but spherical tips are often used due to its simple geometry. Coefficient of friction is determined by the ratio of the frictional force to the loading force on the pin. This test is typically used for low friction coatings such as diamond-like carbon coatings on valve train components in internal combustion engines [17, 18].

Finally, the last analytical technique that could help understand the kinetics of this reaction would be using the Transmission Electron Microscope (TEM). This is an electron microscope like the SEM, but the main difference is that with a TEM, electrons pass through the specimen and reveal an image whereas with a SEM, electrons react with only the surface atoms to provide a picture. Using a TEM would give some insight into what stage of intercalation is commonly seen in the final material and how the copper atoms interact with the carbon atoms [19]. Carbon atoms have a flat hexagonal structure which could allow an entire layer of copper atoms to squeeze between two graphite layers. Another interesting feature would be to see if the intercalation stage is homogeneous or if it changes regularly. Understanding the interaction that takes place at the atomic level could lead to advancements in many other fields related to both carbon and copper related applications.

Even though this project still has work left to do, it relates to a set of problems that engineers deal with regularly in a professional environment. One must be flexible and innovative to work through unforeseen issues in design and environment limitations. Conducting a research project allows for the creation of new skills and knowledge to all

those involved by being exposed to new equipment and real-world applications. Overall, the outlook on the future of this project and the results to date has been very beneficial both personally and professionally.

REFERENCES

[1] Brain, M. "How Electric Motors Work". 01 April 2000. HowStuffWorks.com. <http://electronics.howstuffworks.com/motor.htm> 17 November 2012.

[2] Focus Technology Co., Ltd. Made-in-China.com. <http://a7451414.en.made-in-china.com/product/TezJSpkPgqcV/China-Electric-Motor-Brush.html> 17 November 2012.

[3] Schunk Graphite Technology, LLC. “About Us”. <http://www.schunkgraphite.com/> 17 November 2012.

[4] Dresselhaust, M.S. & Dresselhaust, G. “Intercalation Compounds of Graphite” 29 July 1980. Advances in Physics. <mgm.mit.edu/papers/w959.pdf> 12 November 2012.

[5] Bin, X. et al. “Preparation and Structural Investigation of CuCl2 Graphite Intercalation Compounds”. Acta Geologica Sinica - English Edition. Volume 82, Issue 5, pp. 1056–1060, October 2008.

[6] Find, J. et al. “A New Three-Dimensional Structural Model for the CuCl2 Graphite Intercalation Compound”. Carbon. Volume 37, Issue 9, pp. 1431–1441, 1999.

[7] Bin, X., Chen, J., & Cao, H. “Controlled Growth of Two-Dimensional Copper Nanoplates in Graphite Gallery”. Turk J Chem. Volume 35, pp.181 – 188, 2011.

[8] Inagaki, M. & Ohira, M. “Formation Process of CuCl2-NiCl2-Graphite Intercalation Compounds”. J Mater. Res. Volume 5, Issue 8, August 1990.

[9] Colorado State University. “Thermogravimetric Analysis (TGA)”. <http://www1.chm.colostate.edu/Files/CIFDSC/TGA-MS.pdf> 17 November 2012.

[10] PerkinElmer, Inc. "Frequently Asked Questions: Thermogravimetric Analysis (TGS)". < http://www.perkinelmer.com/CMSResources/Images/44-74556GDE_TGABeginnersGuide.pdf> 17 November 2012.

[11] Portland State University. “X-Ray Diffraction”. <http://web.pdx.edu/~pmoeck/phy381/Topic5a-XRD.pdf> 17 November 2012.

[12] PDF Card from AAF

[13] Brunauer, S. et al., J. Am. Chem. Soc., 1938, 60, 309.

[14] Barrett, E. P. et al. “The Determination of Pore Volume and Area Distributions in Porous Substances”. Computations from Nitrogen Isotherms // J. Am. Chem. Soc. 1951. V. 73. P. 373–380.

[15] Nanoindentation Lecture 1 Basic Principle, by Do Kyung Kim, Dept. of Material Science and Engineering KAIST, Korea.

[16] Fischer-Cripps, A.C. Nanoindentation. (Springer: New York), 2004.

[17] Historic scientific instruments in Denmark.

[18] Hutton, C. A Mathematical and Philosophical Dictionary

[19] Nobel Media. “The Transmission Electron Microscope”. <http://www.nobelprize.org/educational/physics/microscopes/tem/index.html 17> 17 November 2012.